DARK MATTER

Around 30 % of the Universe is matter of which ~26-27 % is dark matter.

COMA Cluster

1. >10,000 members, R ~ 3 Mpc, $M \sim 7 \times 10^{14}\ M_o$
2. D ~ 99 Mpc, z = 0.231
3. σ ~ 900 km/s

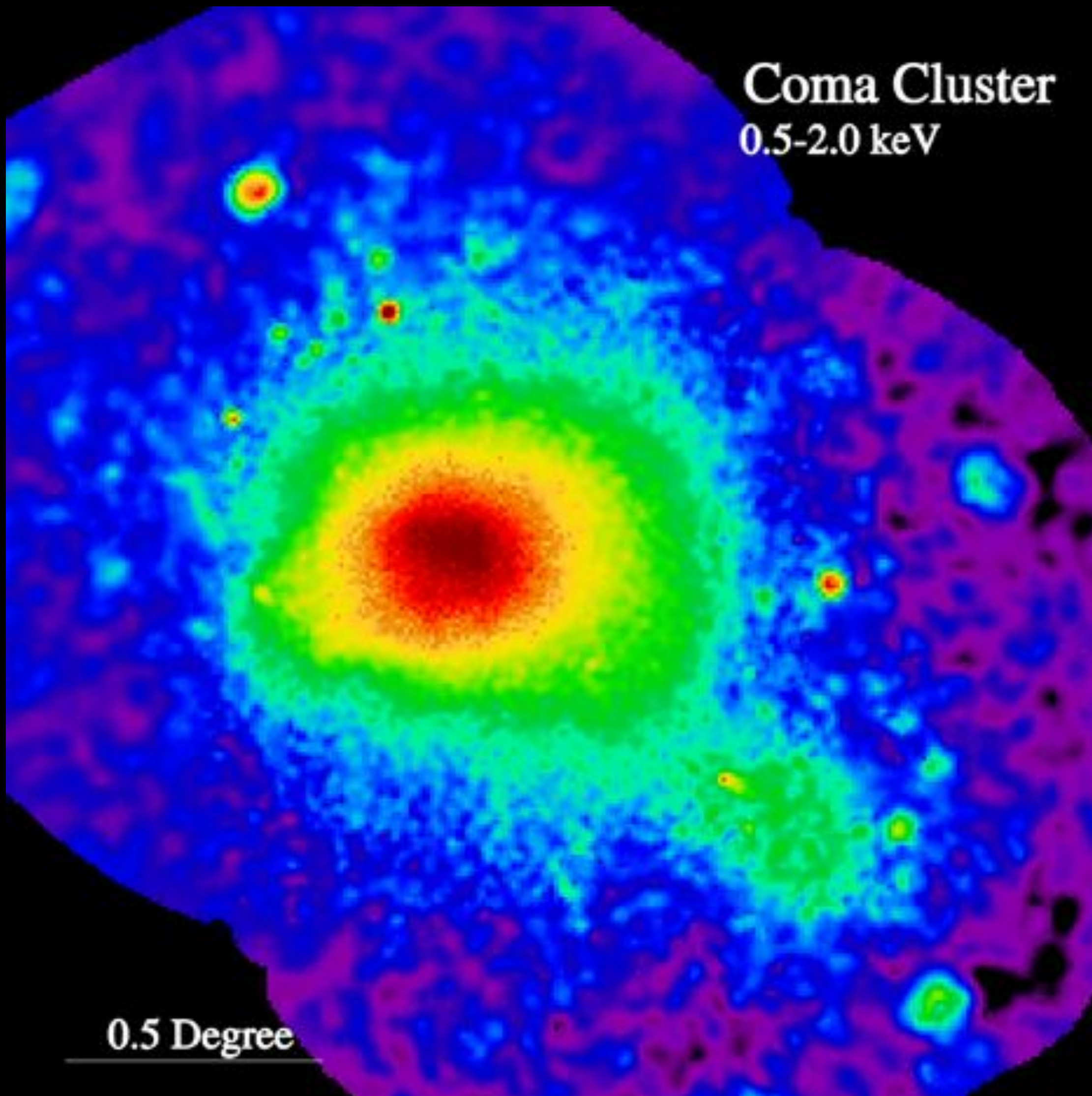

COMA Cluster
Soft x-ray image obtained by ROSAT

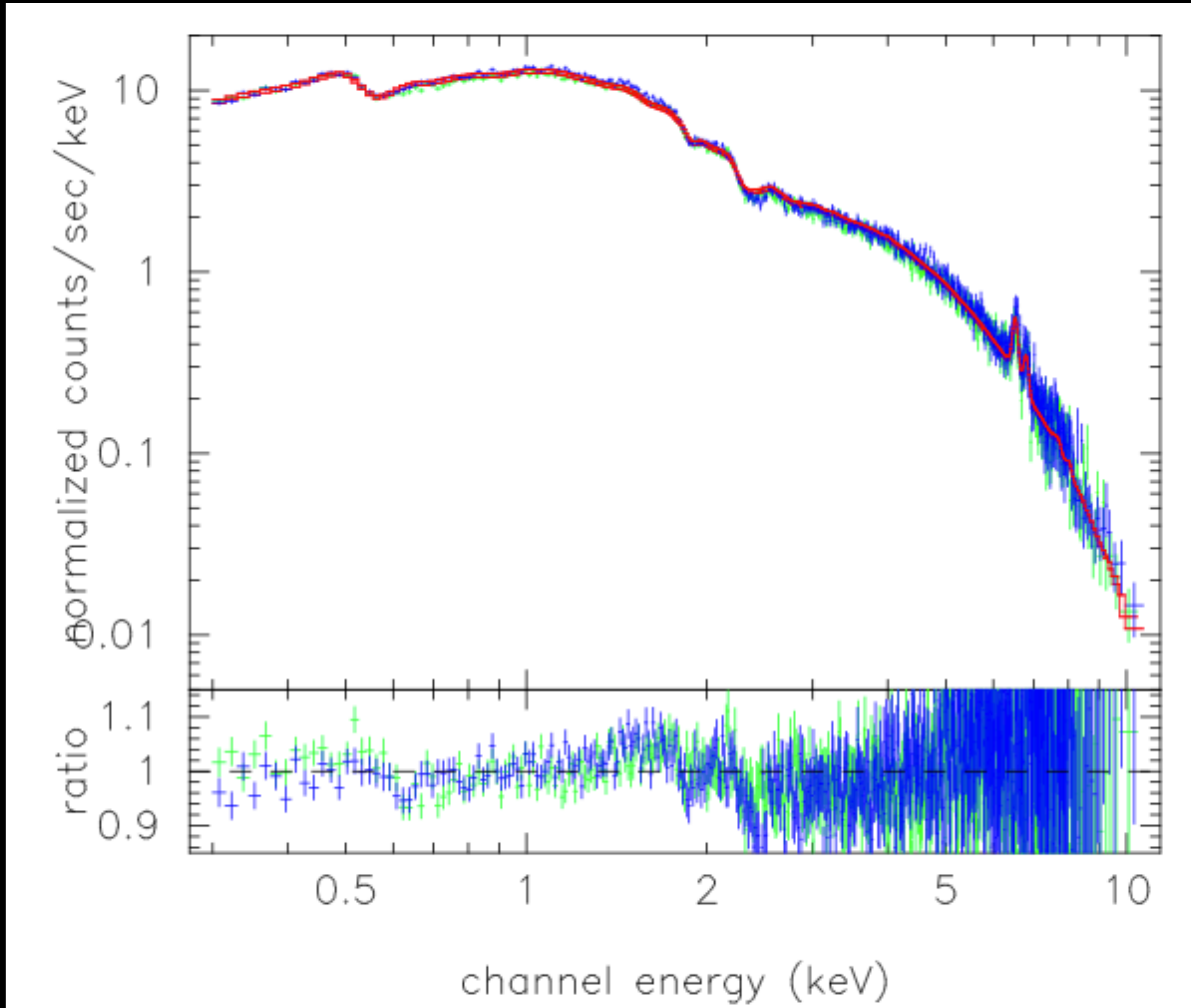

normalized counts/sec/keV
10
1
0.1
0.01
ratio
1.1
1
0.9
0.5
1
2
5
10
channel energy (keV)

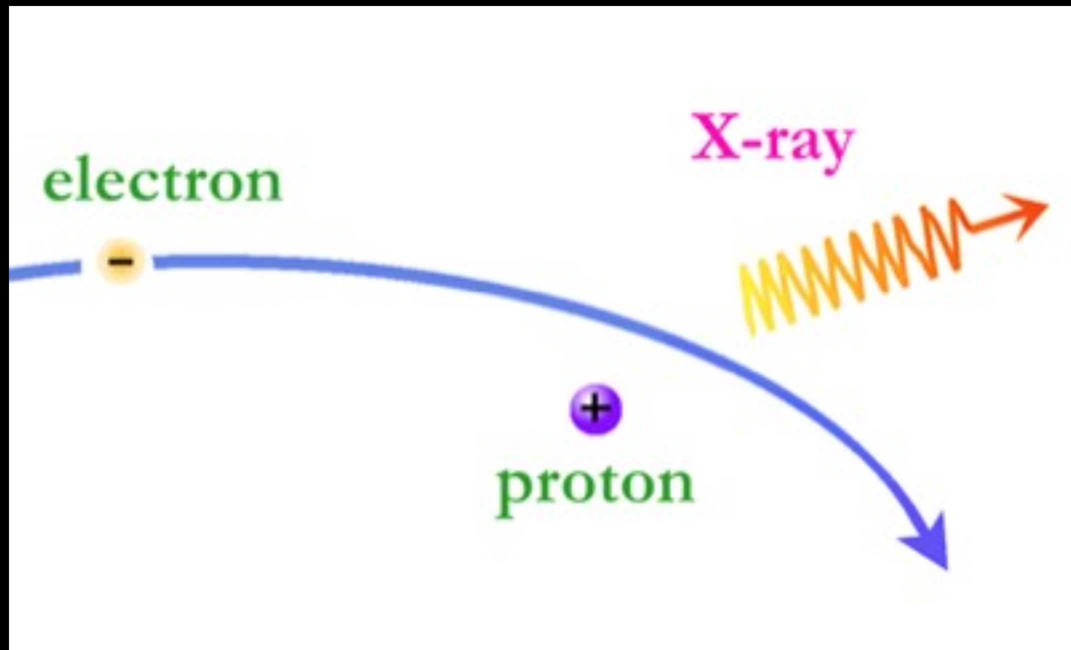

Bremsstrahlung (free-free) Emission

$\varepsilon_\nu = 6.8\text{x}10^{-38} n_e n_i Z^2 g_{ff} T^{-1/2} e\text{-}h\nu/kT$ erg s^{-1} cm-3 Hz^{-1}

$\varepsilon = 2.4\text{x}10^{-27} n_e n_i Z^2 g_{ff} T^{1/2}$ erg s^{-1} cm^{-3}

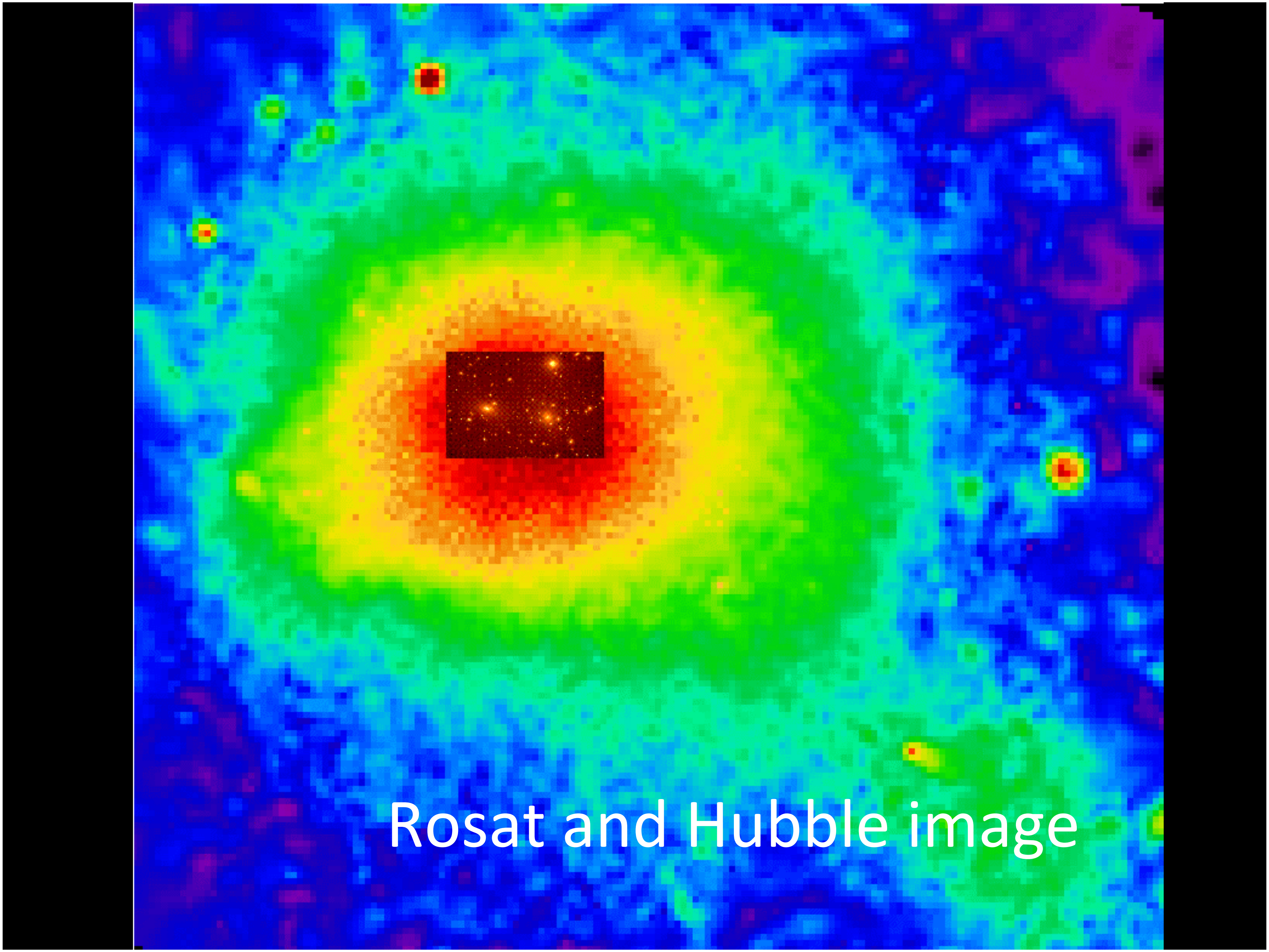
Rosat and Hubble image

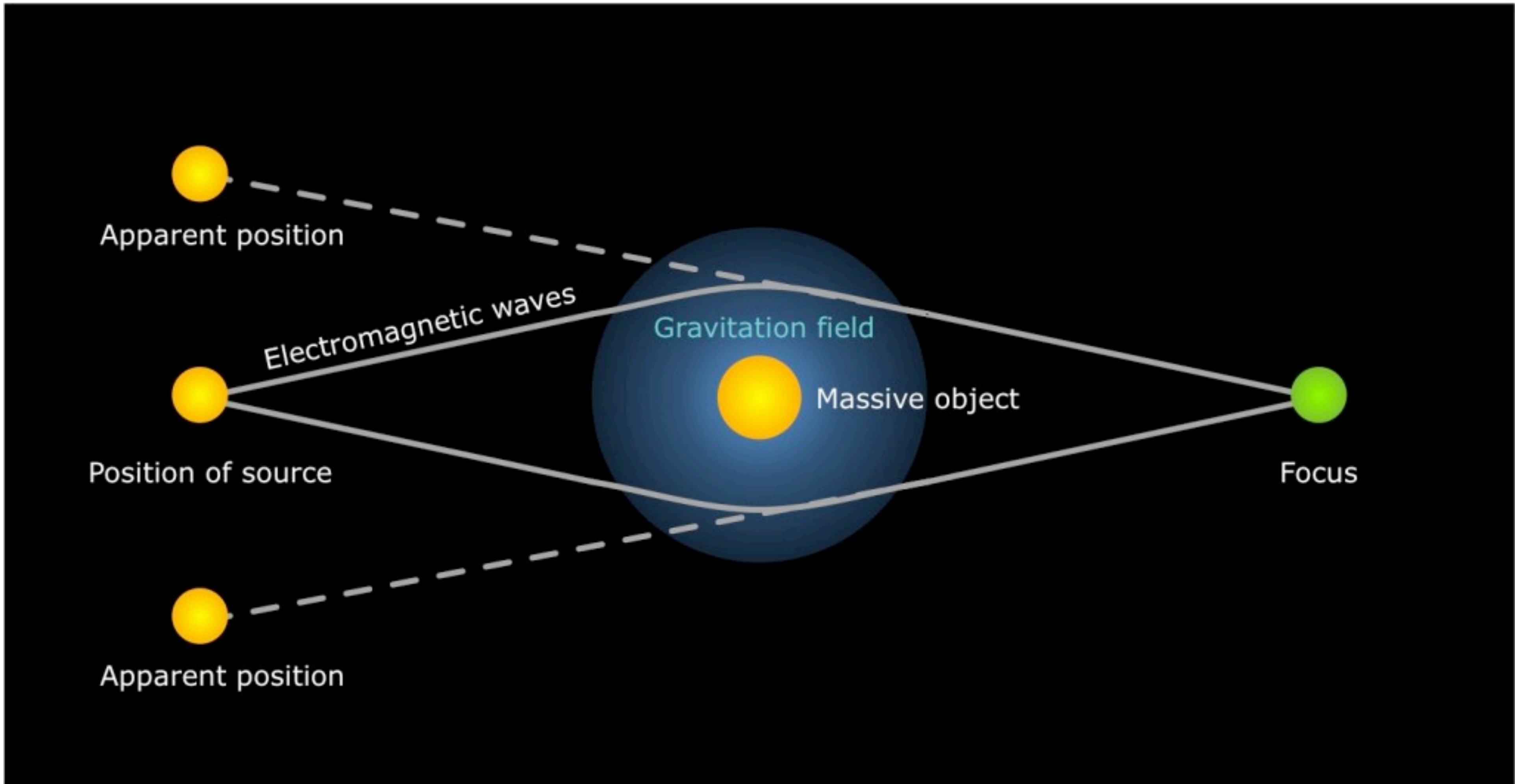

Schematic of Gravitational Lensing

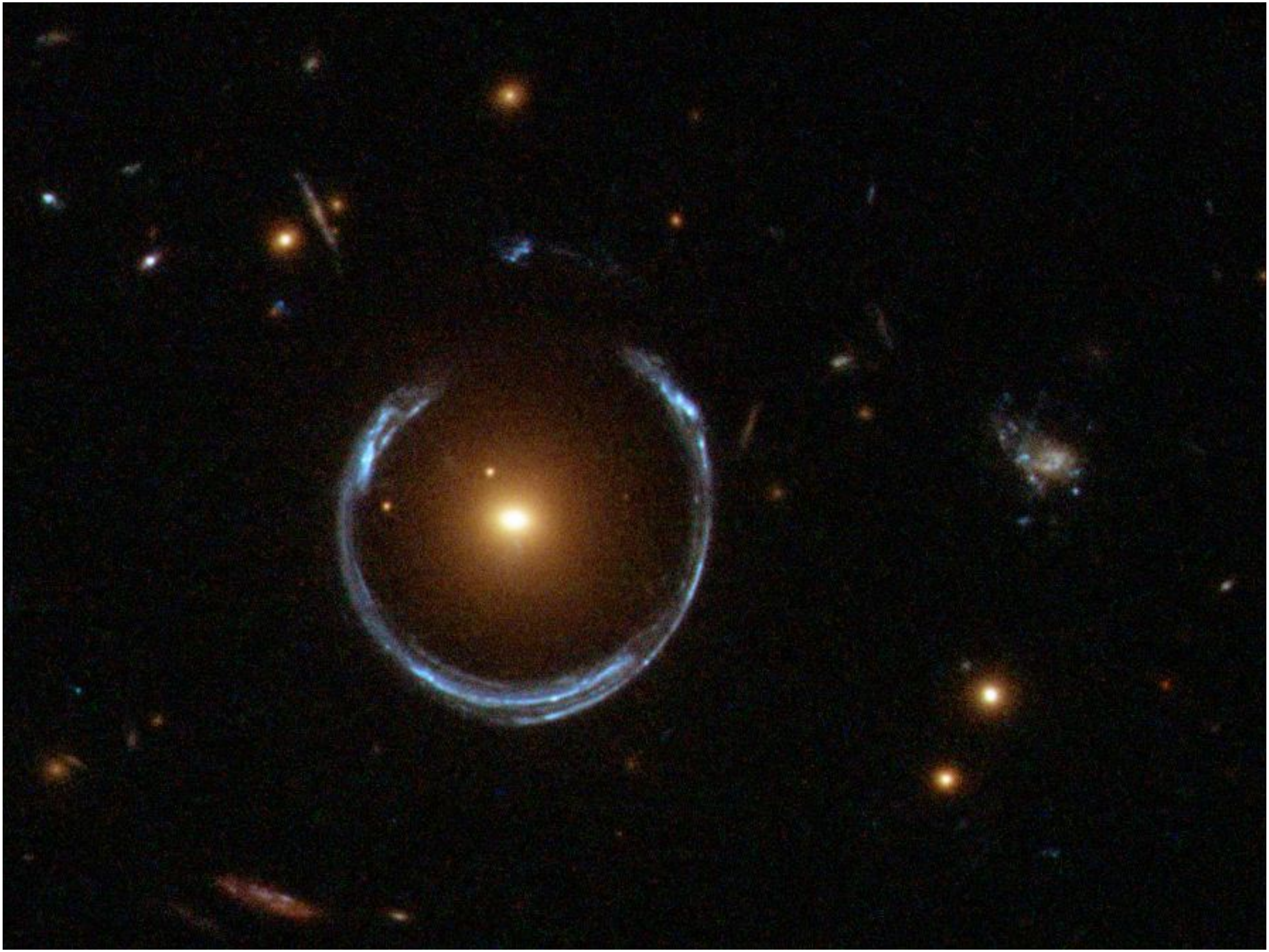

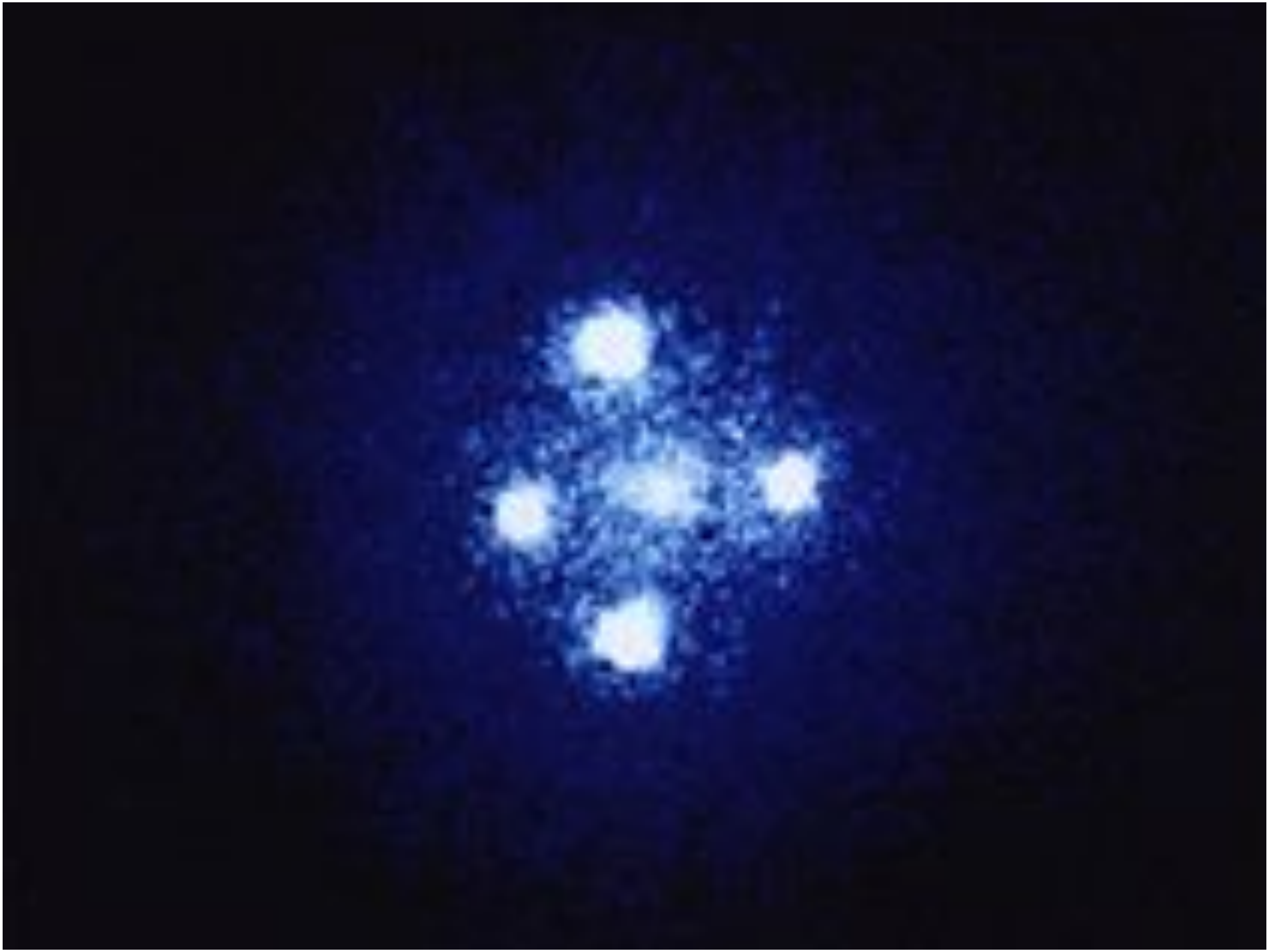

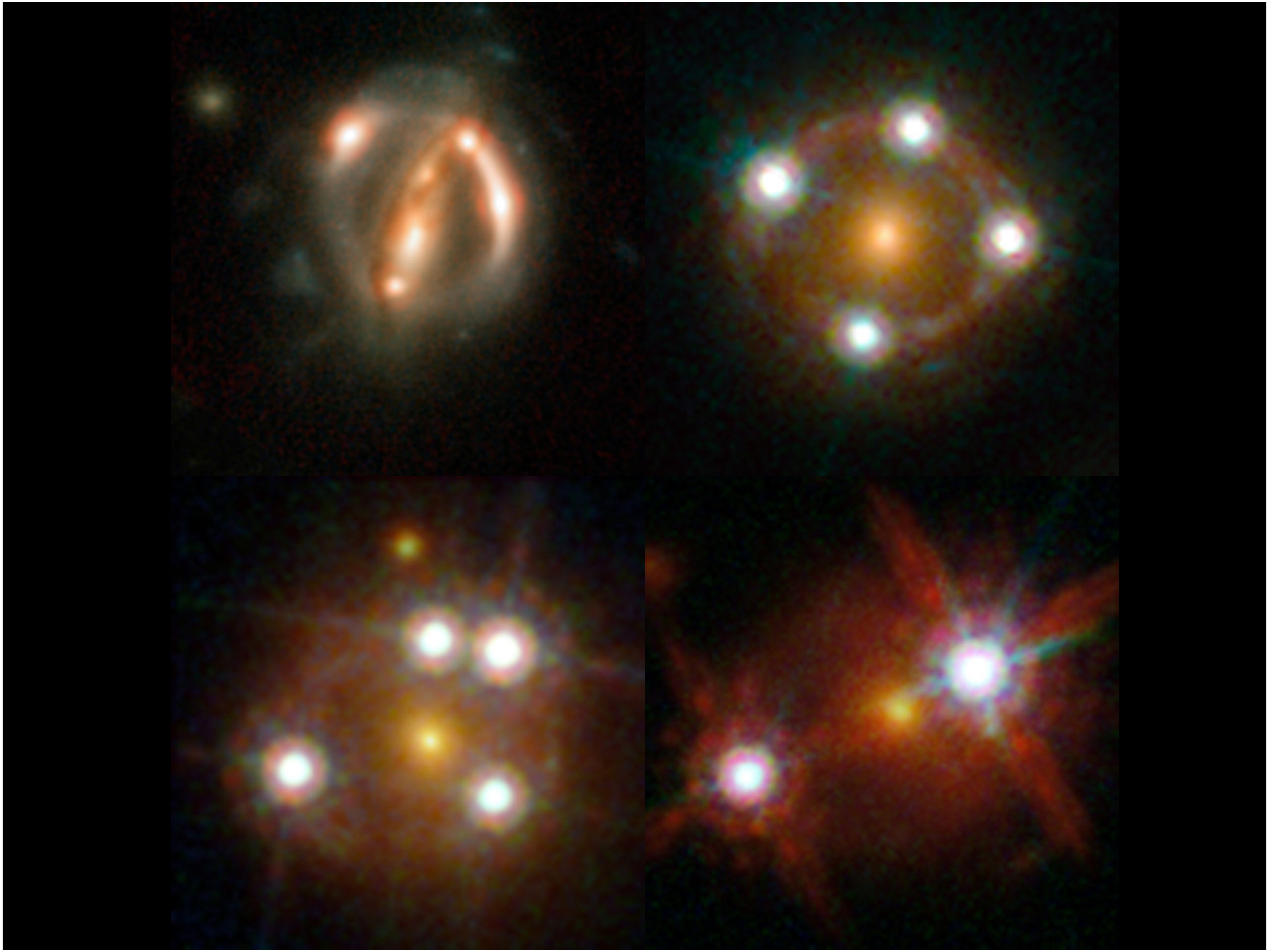

Distant Galaxy Lensed by Cluster Abell 2218
Hubble Space Telescope • WFPC2 • ACS

ESA, NASA, J.-P. Kneib (Caltech/Observatoire Midi-Pyrénées) and R. Ellis (Caltech) STScI-PRC04-08

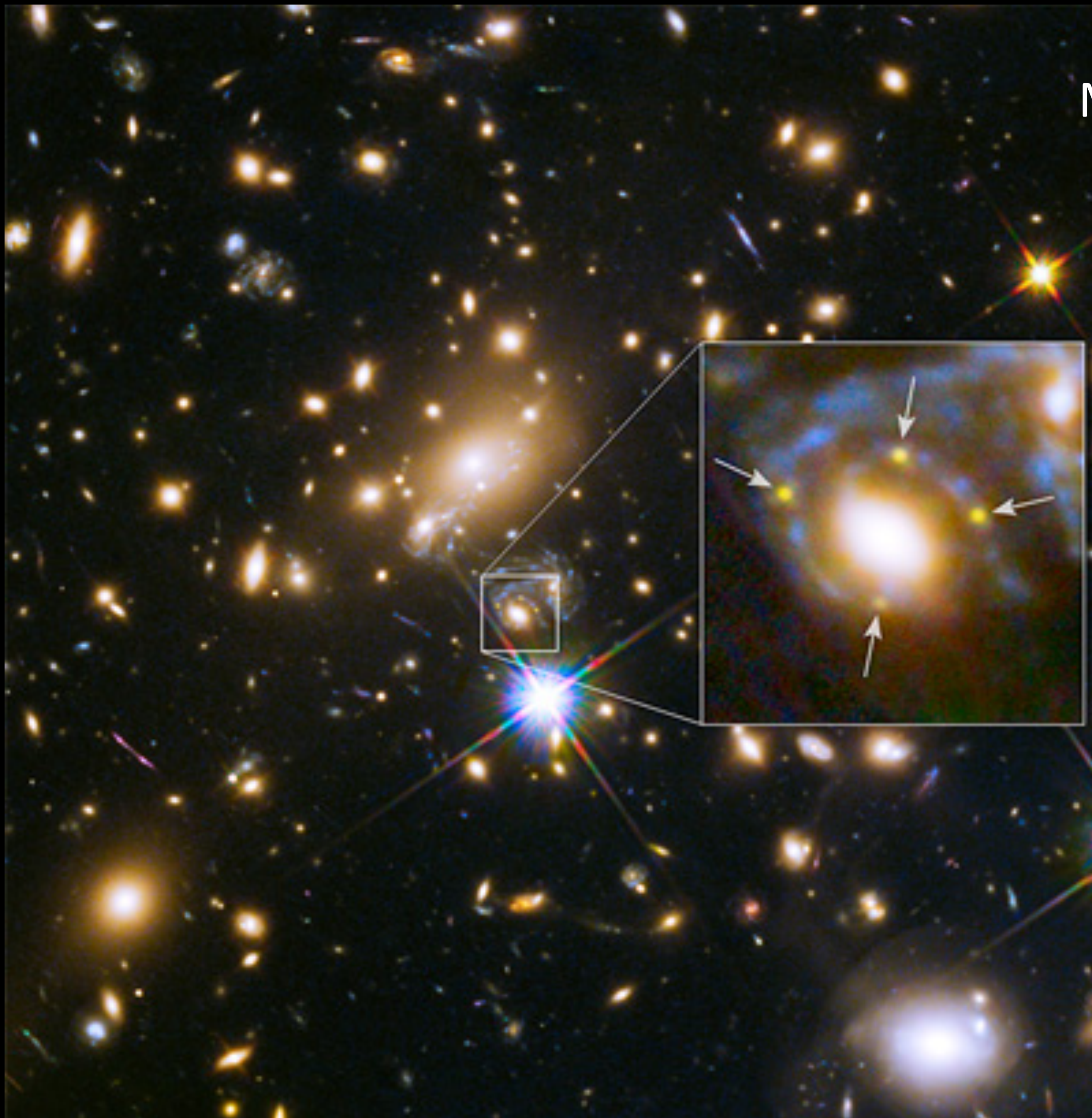

MACS J1149.6+2223 lenses background Supernova

Rotation Curves

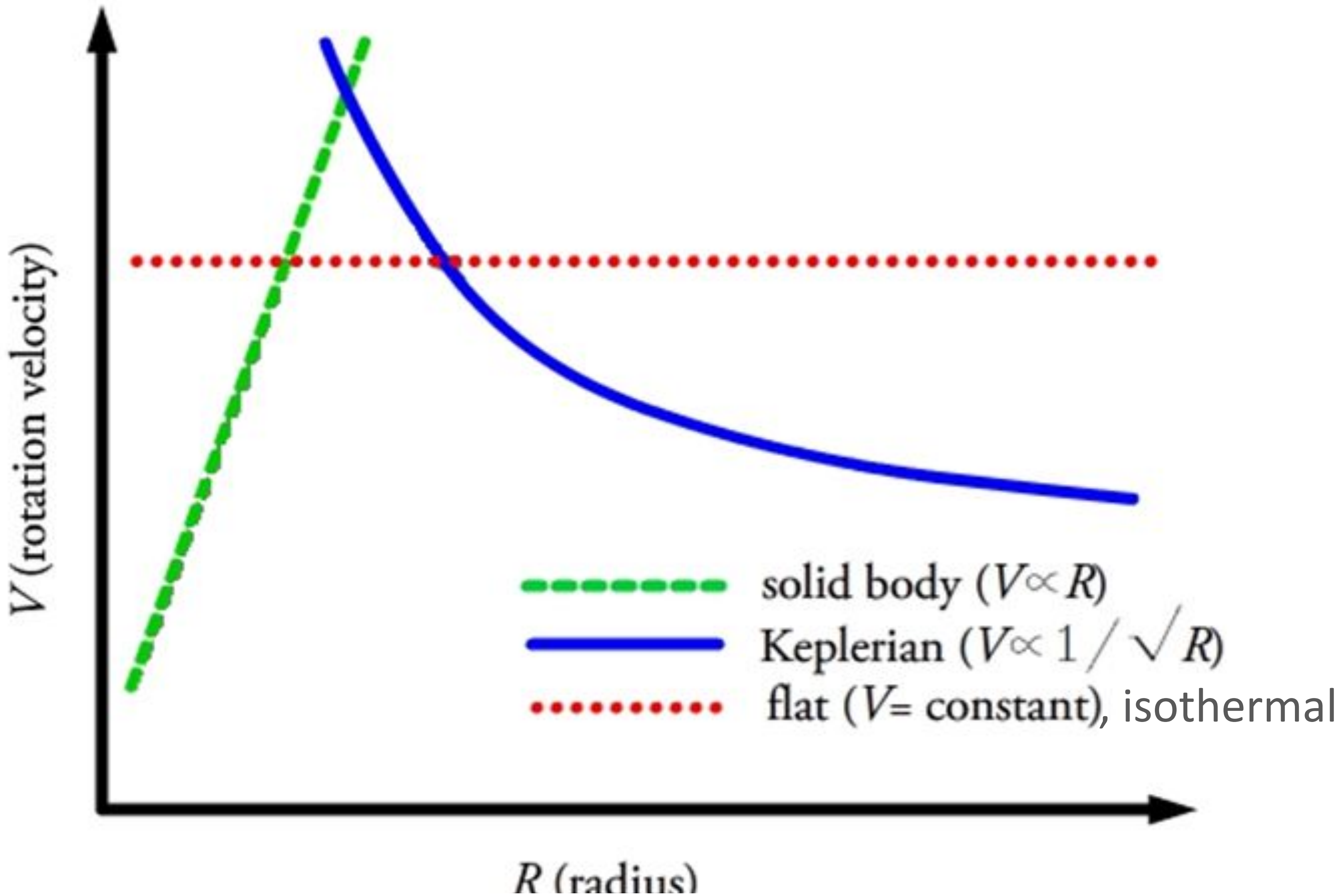

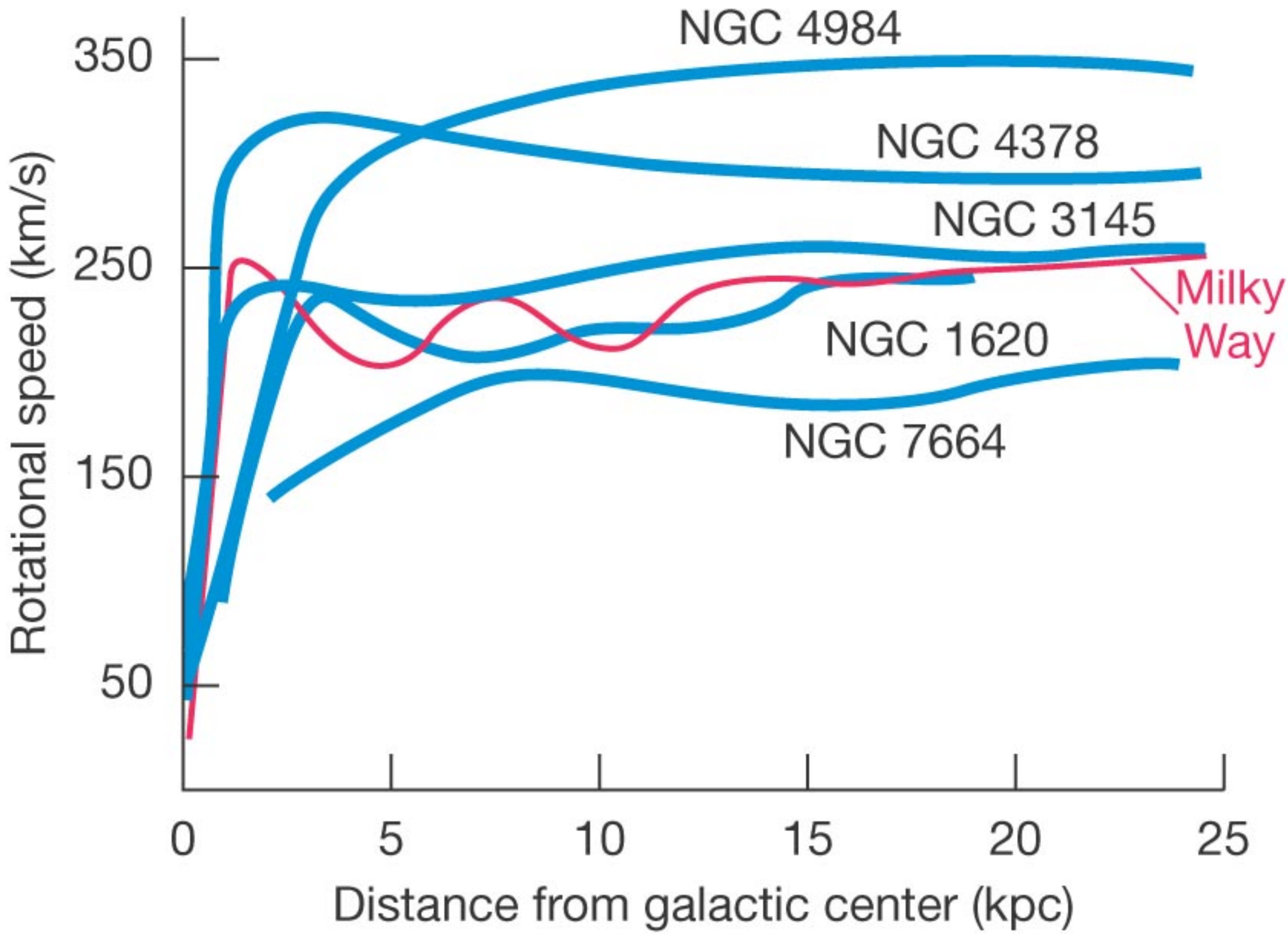
NGC 4984
NGC 4378
NGC 3145
Milky Way
NGC 1620
NGC 7664
350
250
150
50
Rotational speed (km/s)
0
5
10
15
20
25
Distance from galactic center (kpc)
(b)

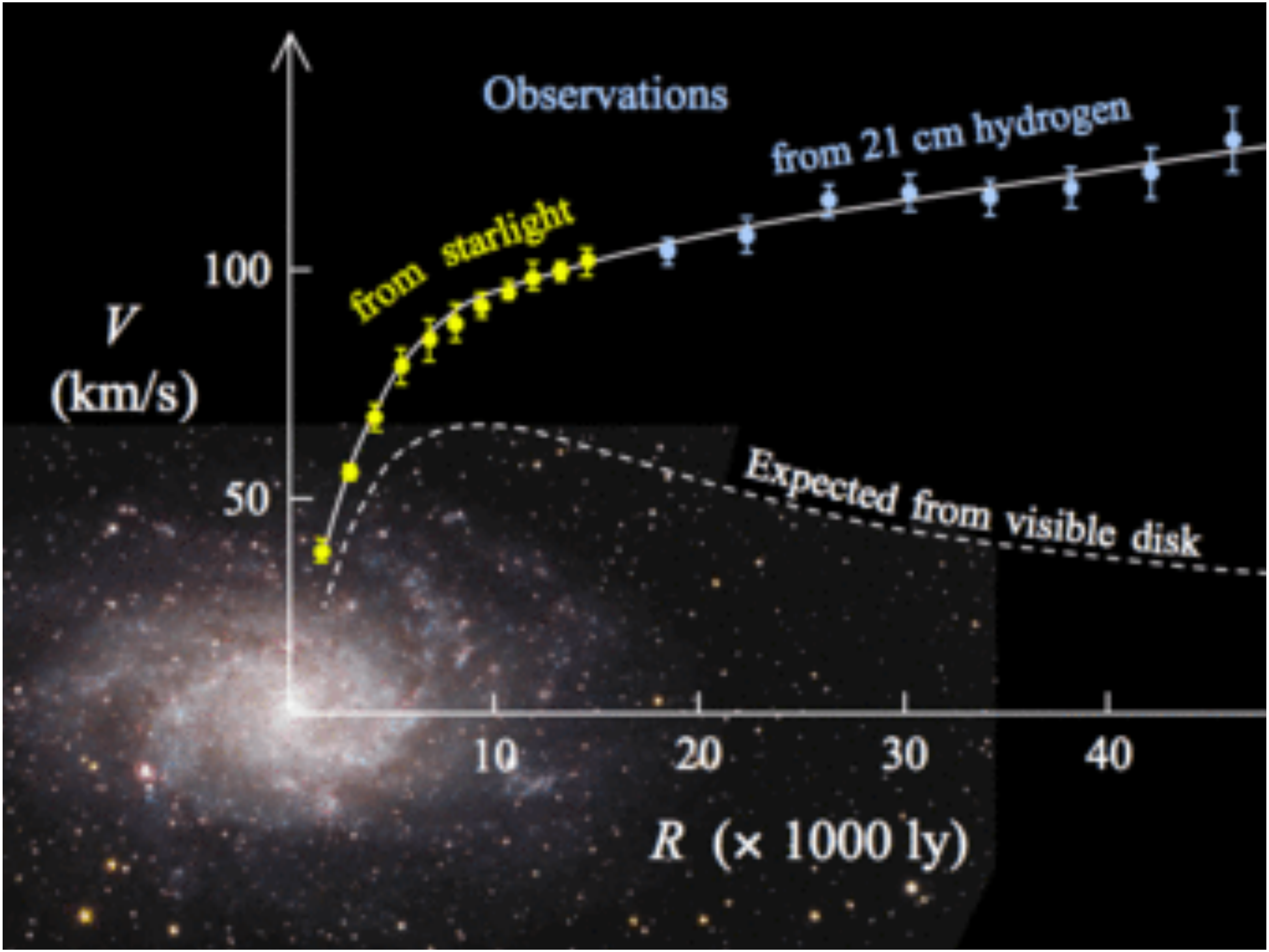
Observations
from 21 cm hydrogen
from starlight
100
V
(km/s)
50
Expected from visible disk
10
20
30
40
R (× 1000 ly)

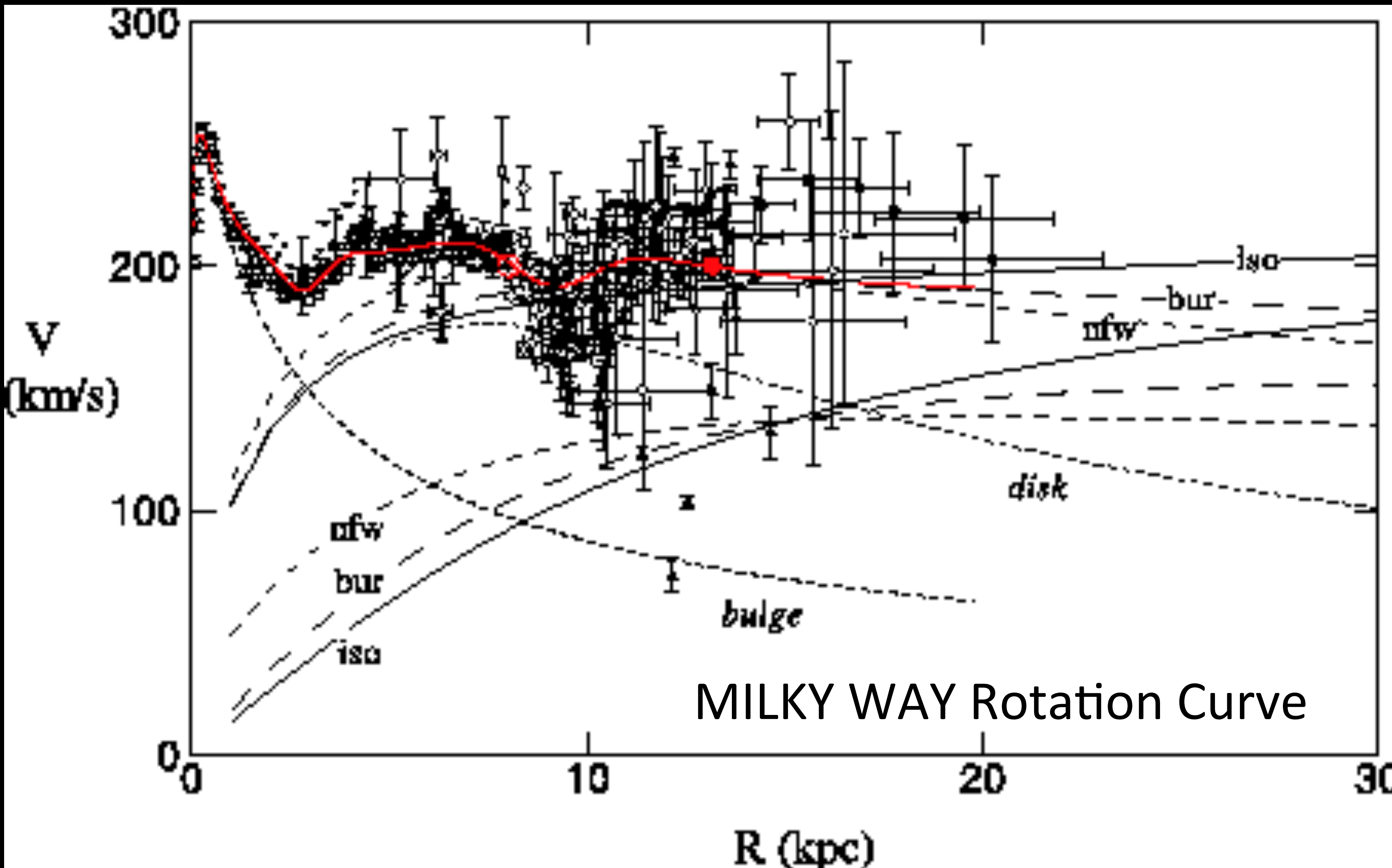

300
200
100
0
V
(km/s)
0
10
20
30
R (kpc)
iso
bur
nfw
disk
bulge
MILKY WAY Rotation Curve

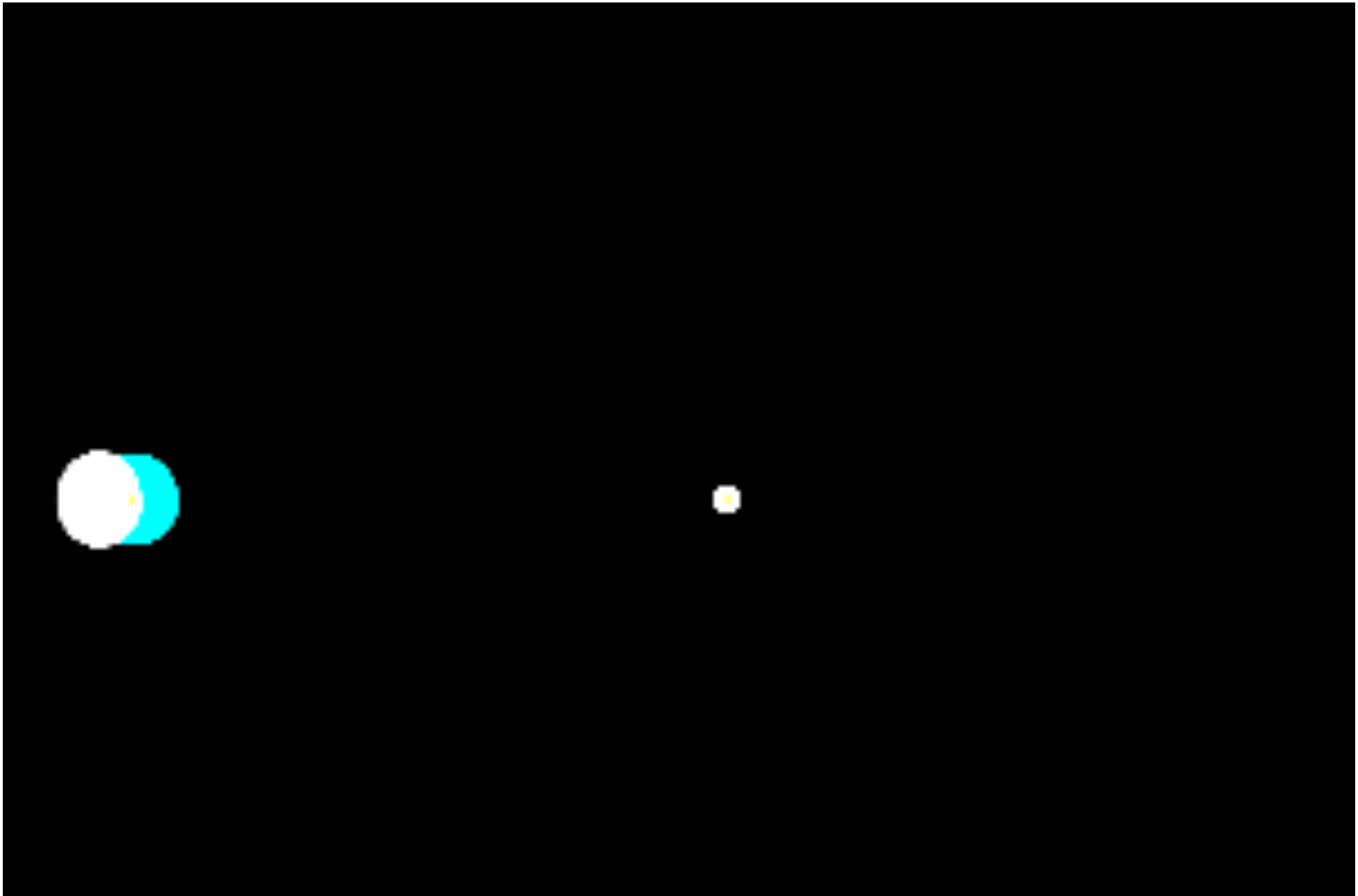

Passage of a MACHO in front of a distant star

MACHO Results

Analysis of 5.7 years of photometry on 11.9 million stars in the LMC reveals 13 -17 microlensing events. A detailed treatment of our detection efficiency shows that this is significantly more than the 2 to 4 events expected from lensing by known stellar populations. The timescales of the events range from 34 to 230 days. We estimate the microlensing optical depth towards the LMC from events with $2 < t < 400$ days to be 1.2×10^{-7} with an additional 20%-30% systematic error. The spatial distribution of events is mildly inconsistent with LMC/LMC disk self-lensing, but is consistent with an extended lens distribution such as a Milky Way or LMC halo. Interpreted in the context of a Galactic dark matter halo, consisting partially of compact objects, a maximum likelihood analysis gives MACHO halo fraction of 20% for a typical halo model with a 95% confidence interval of 8% to 50%. A 100% MACHO halo is ruled out at the 95% C.L. for all except our most e xtreme halo model. Interpreted as a Galactic halo population, the most likely MACHO mass is between 0.15 and 0.9 Solar masses, depending on the halo model, and the total mass in MACHOs outto 50 kpc is found to be 9×10^{10} , independent of the halo model.

EROS and OGLE Re-Analysis

A new analysis of the results of the EROS-2, OGLE-II, and OGLE-III microlensing campaigns towards the Small Magellanic Cloud (SMC) shed light on the issue of the nature of the reported microlensing candidate events, whether to be attributed to lenses belonging to known population (the SMC luminous components or the Milky Way disc, to which we broadly refer to as "self lensing") or to the would be population of dark matter compact halo objects (MACHOs). Overall, of five reported microlensing events towards the SMC (one by EROS and four by OGLE), the re-analysis shows that in terms of number of events the expected self lensing signal may indeed explain the observed rate. However, the characteristics of the events, spatial distribution and duration (and for one event, the projected velocity) rather suggest a non-self lensing origin for a few of them. In particular the upper limit for the halo mass fraction in form of MACHOs given the expected self-lensing and MACHO lensing signal. At 95% CL, the tighter upper limit, about 10%, is found for MACHO mass of $10-2M_{\odot}$, upper limit that reduces to above 20% for $0.5M_{\odot}$ MACHOs.

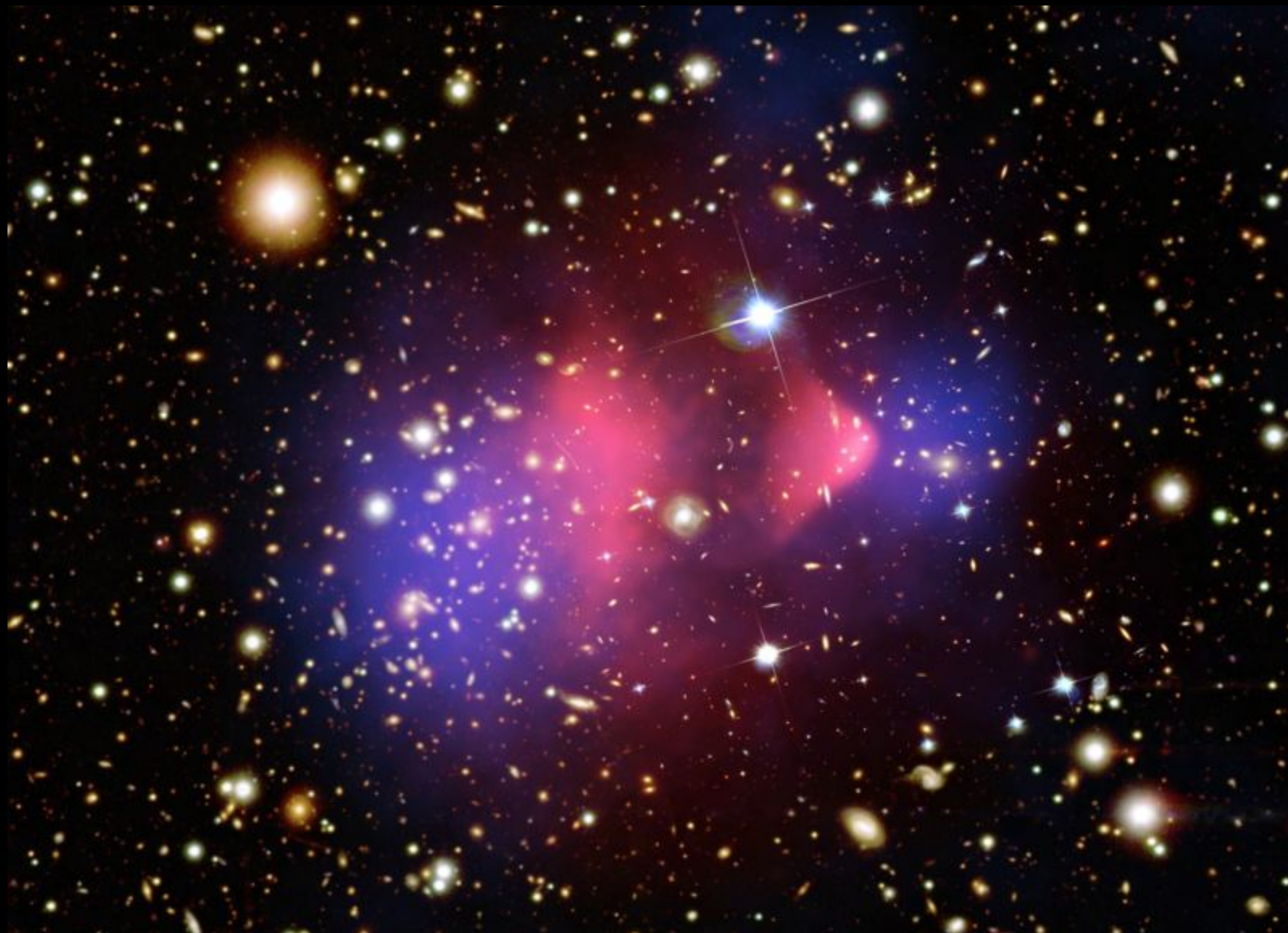

Bullet Cluster (1E0657-558) -- Colliding clusters

1. 40 galaxies
2. z= 0.296,D=1.41 GPc
3. kT=17.4 keV, L_x =1.4x10^{46} erg/s

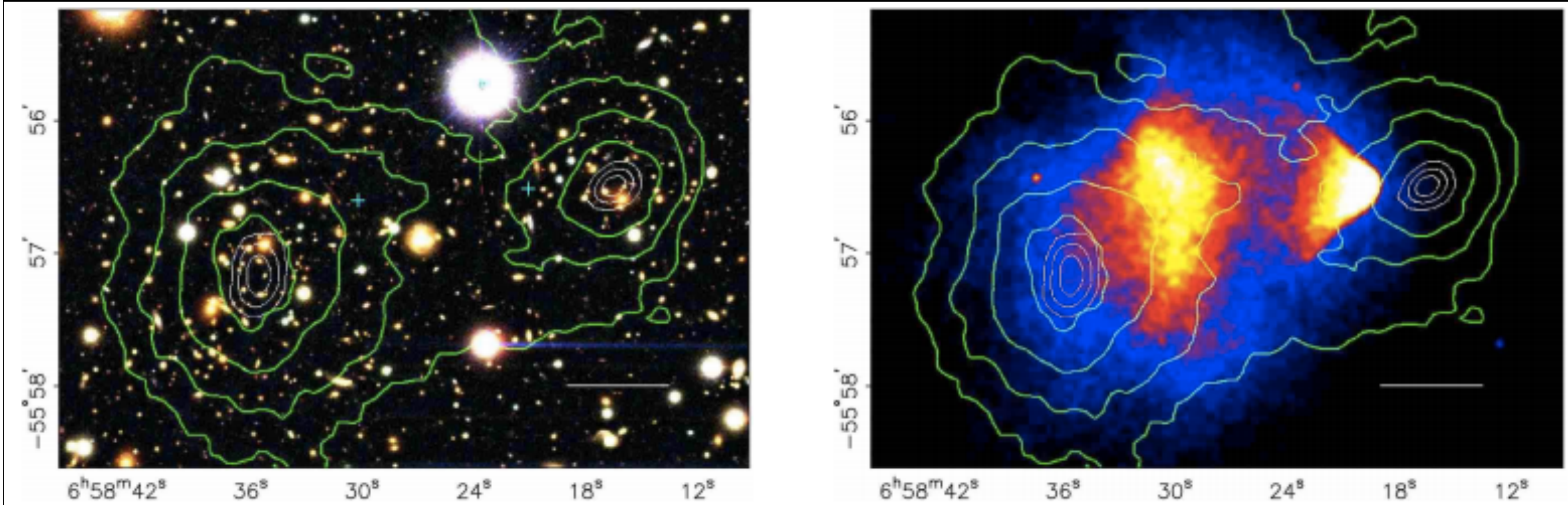

On the left is the dark matter distribution as determined by gravitational lensing
On the right is the x-ray image obtained by the Chandra X-ray Observatory with the mass contours superimposed.

Inferred from the Chandra observations of 1E0657-56, the cluster is undergoing a high-velocity (around 4500 km/s) merger, based on the distribution of the hot, X-ray emitting gas. The dark matter clump, revealed by the weak-lensing map, is coincident with the collisionless galaxies, but lies ahead of the collisional gas.

The velocity of the bullet subcluster is exceptionally high for a cluster substructure, and "cannot be accommodated within the currently favoured Lambda-CDM model cosmology." A later study said the velocities of the collision as currently measured are "compatible with the prediction of a LCDM model." Subsequent work found the collision to be consistent with LCDM simulations. The discrepancies resulted from small simulations and the methodology of identifying pairs. Earlier claims the Bullet Cluster was inconsistent with standard cosmology was based on an erroneous estimate of the speed of the shock in the X-ray emitting gas.

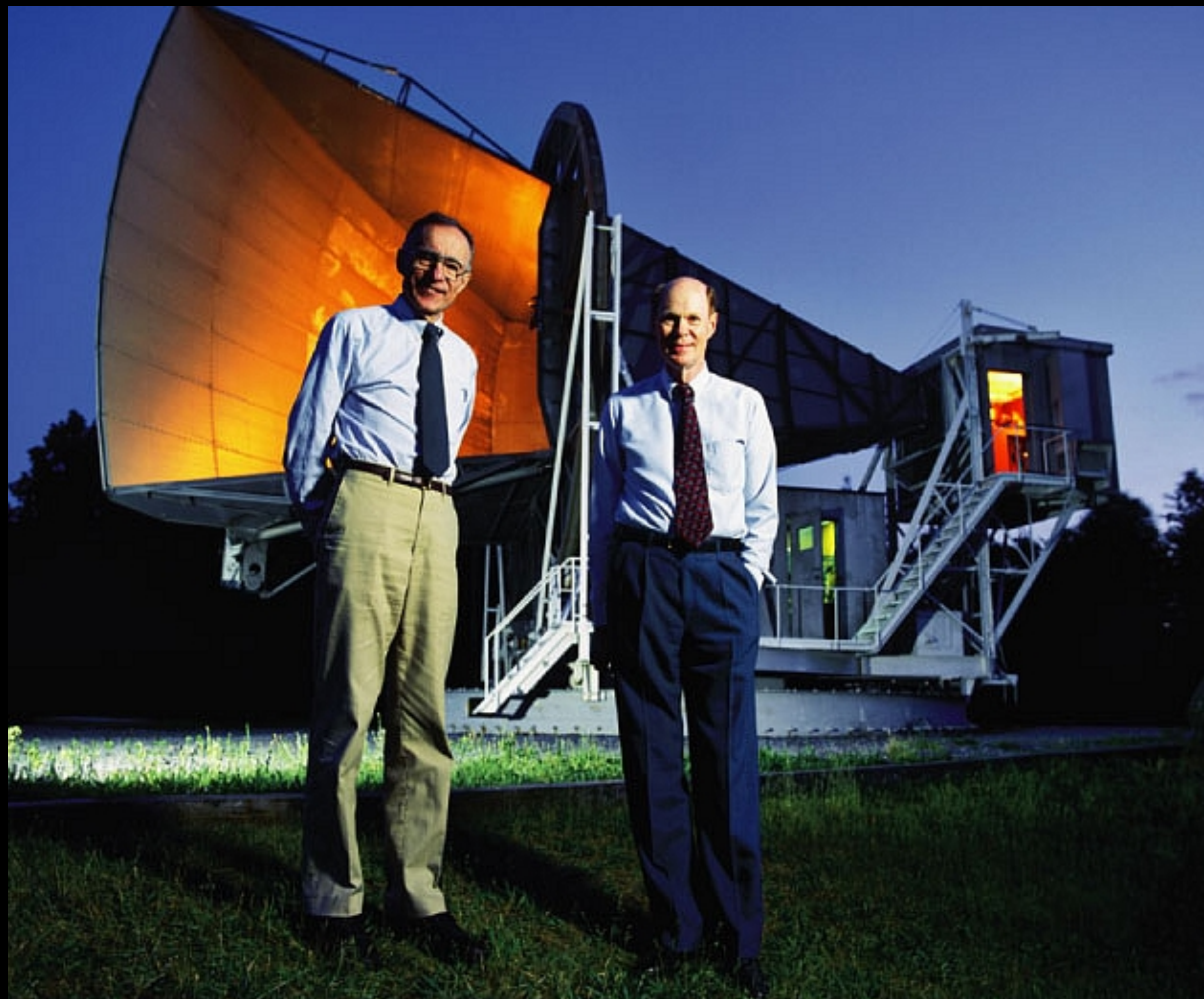

COSMIC MICROWAVE BACKGROUND RADIATION (CMB)

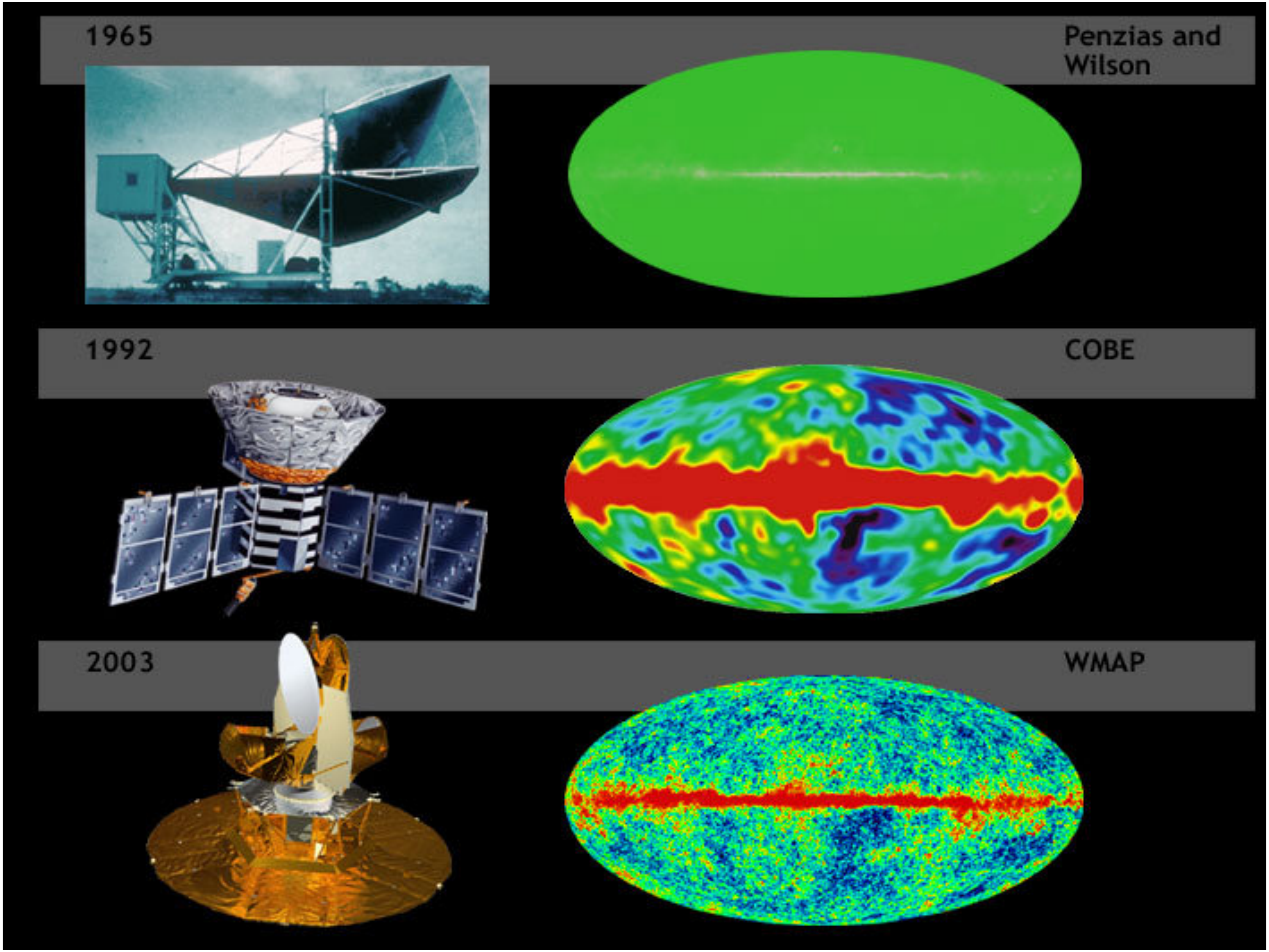
1965
Penzias and Wilson
1992
COBE
2003
WMAP

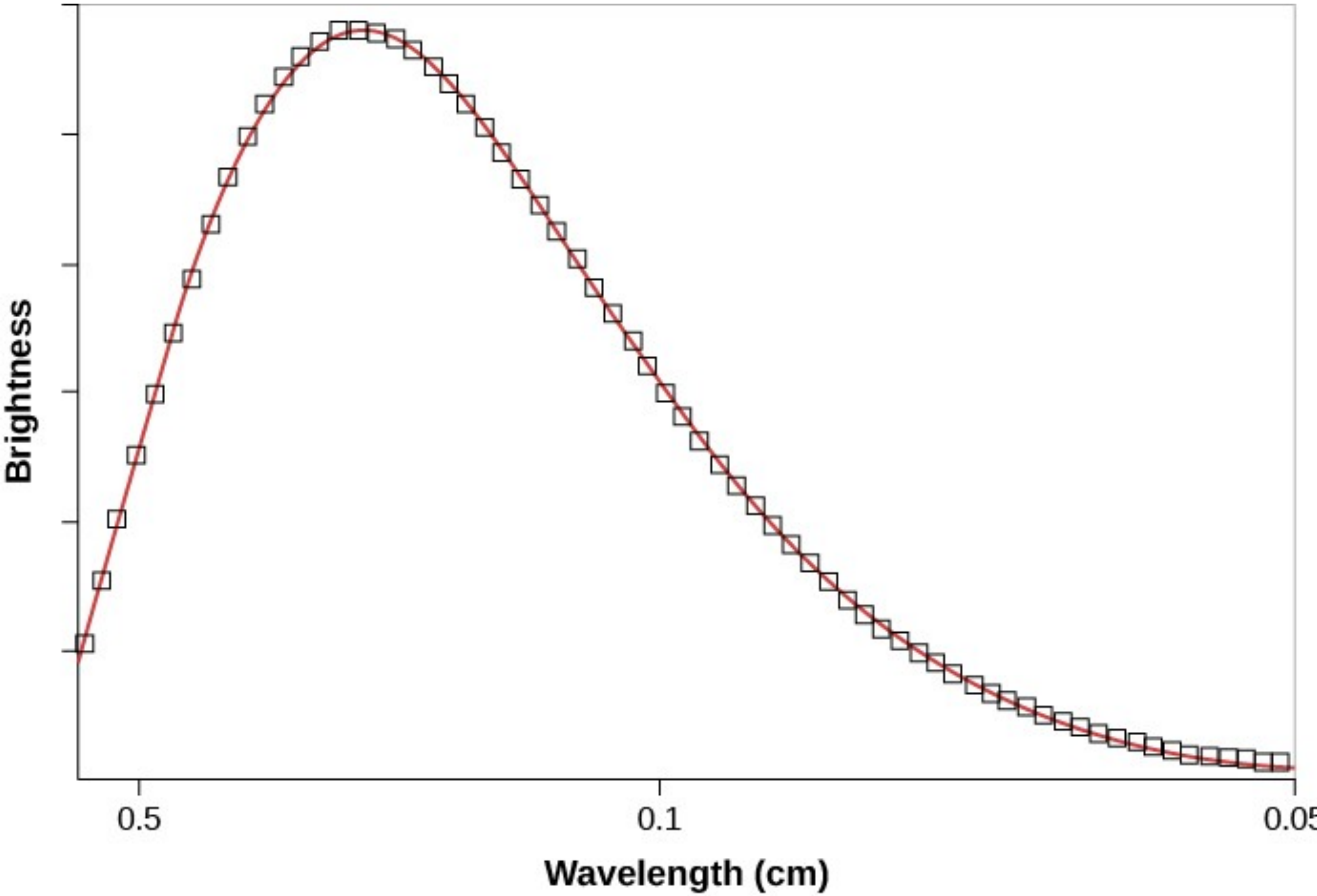

The spectrum of the CMBR is blackbody in shape with temperature
T = 2.725 K and is nearly isotropic except for some well-known distortions.

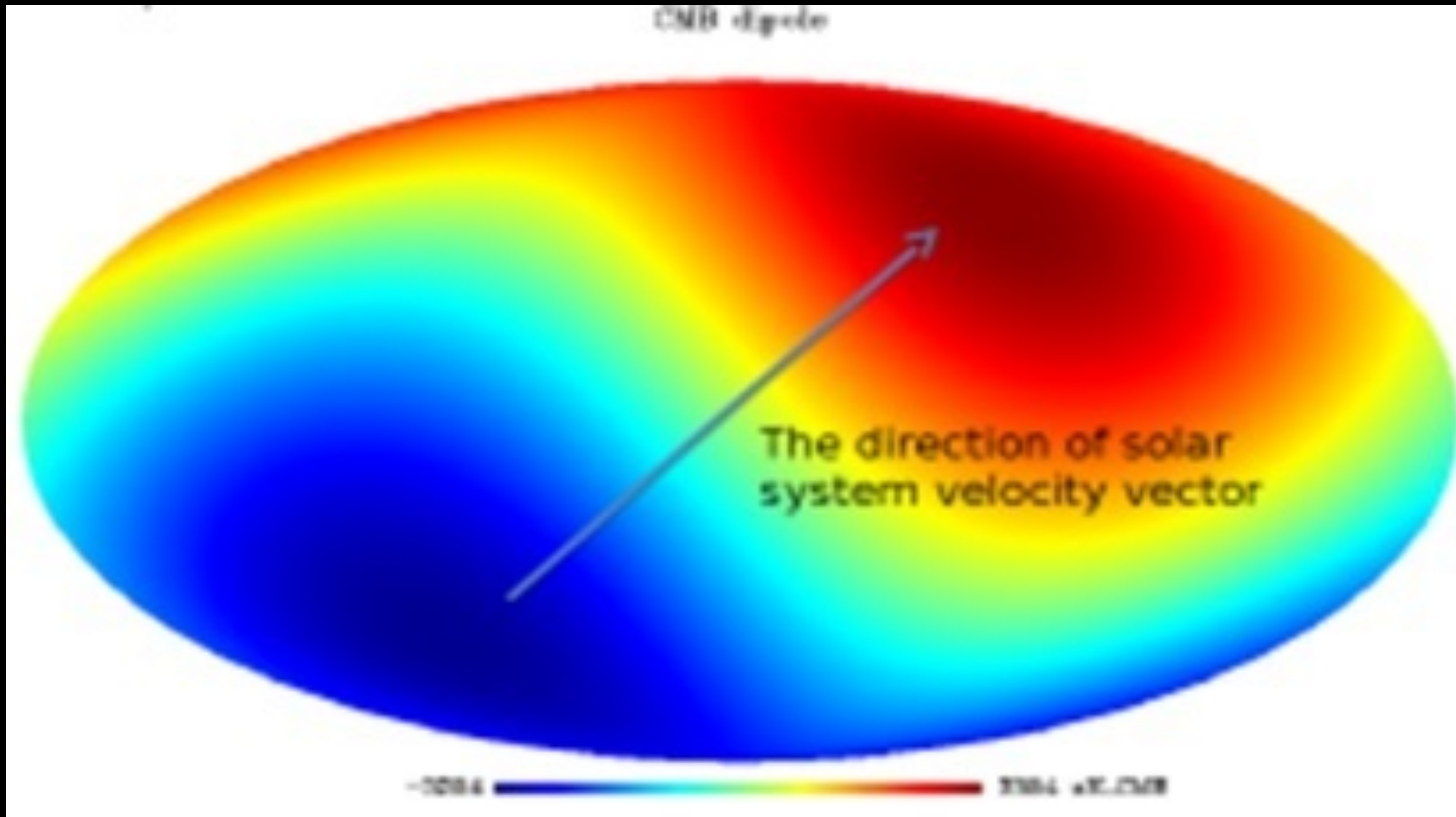

Dipole Anisotropy, $\delta T = 0.0035$ K → $v = 0.002c$ in direction of Hydra

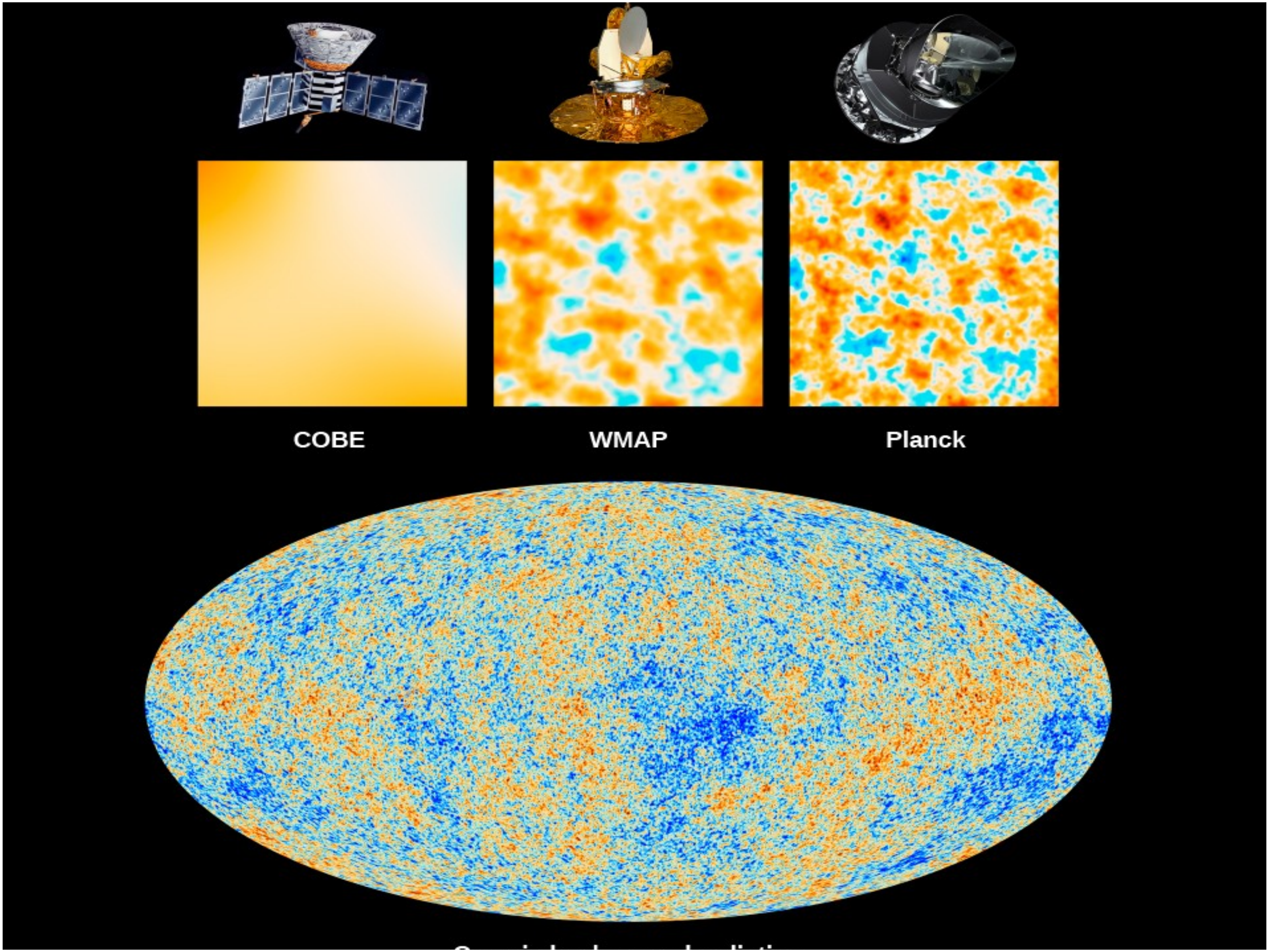
COBE
WMAP
Planck

$$T = 2.725^\circ K, \quad \frac{\delta T}{T} \sim 10^{-5}$$

WMAP

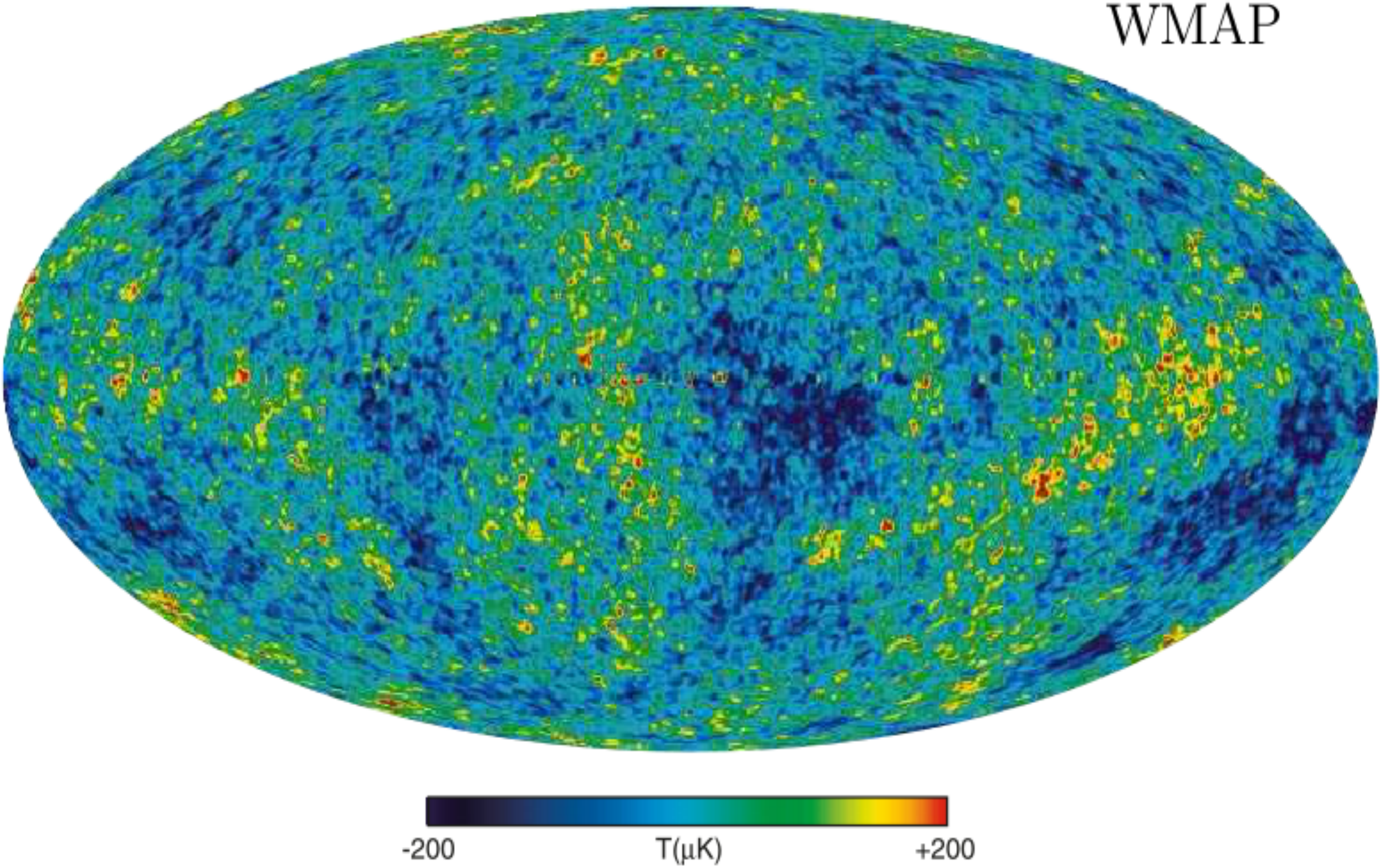

Fourier Analysis

$$g(t) = a_0 + \sum_{m=1}^{\infty} a_m \cos\left(\frac{2\pi mt}{T}\right) + \sum_{n=1}^{\infty} b_n \sin\left(\frac{2\pi nt}{T}\right)$$

$$= \sum_{m=0}^{\infty} a_m \cos\left(\frac{2\pi mt}{T}\right) + \sum_{n=1}^{\infty} b_n \sin\left(\frac{2\pi nt}{T}\right)$$

- Fitting a Fourier series to long strings of unevenly spaced data is straightforward, but inefficient from a computational standpoint. The work scales as N^2 where N is the number of data points
- When the data points are evenly spaced, the numerical problem has a clever solution, the so-called the FAST FOURIER TRANSFORM (FFT) which, IMO, is the computer algorithm of the last 100 years. The FFT scales as $N \log_e N \ll N^2$ for large N.
- Application of the FFT to the data below allows a rapid decomposition of the time series showing that a seemingly random process is actually a linear combination of a small number of waves

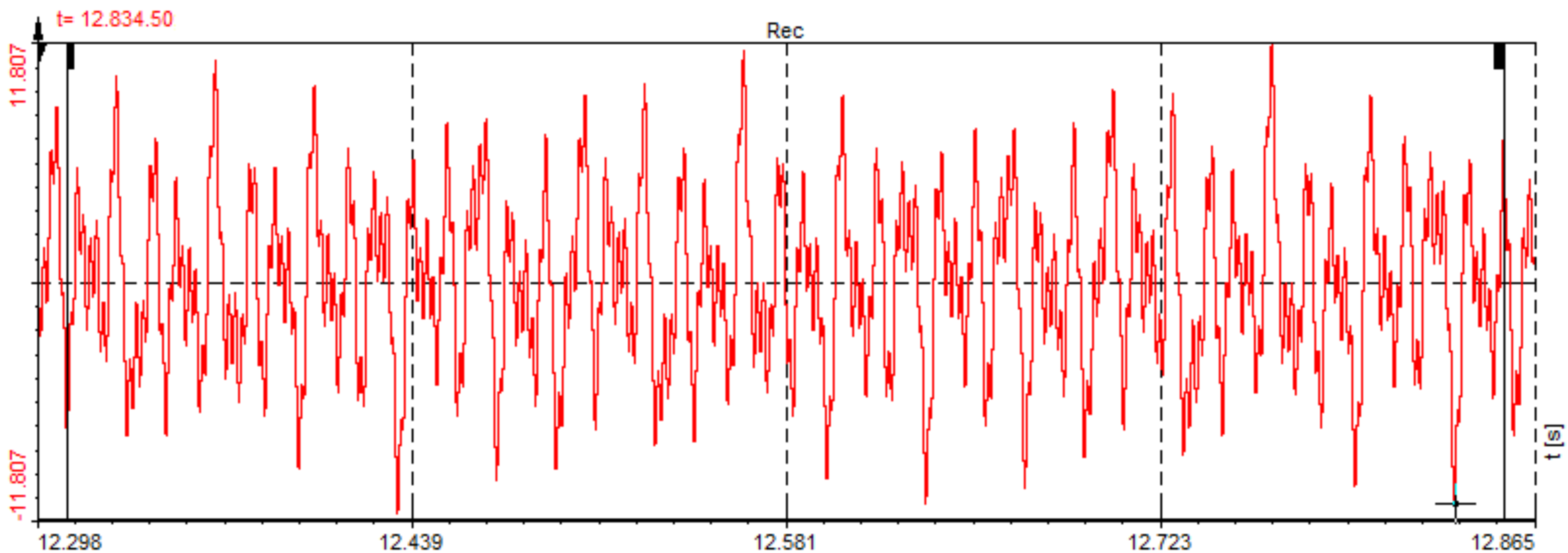

[redacted]

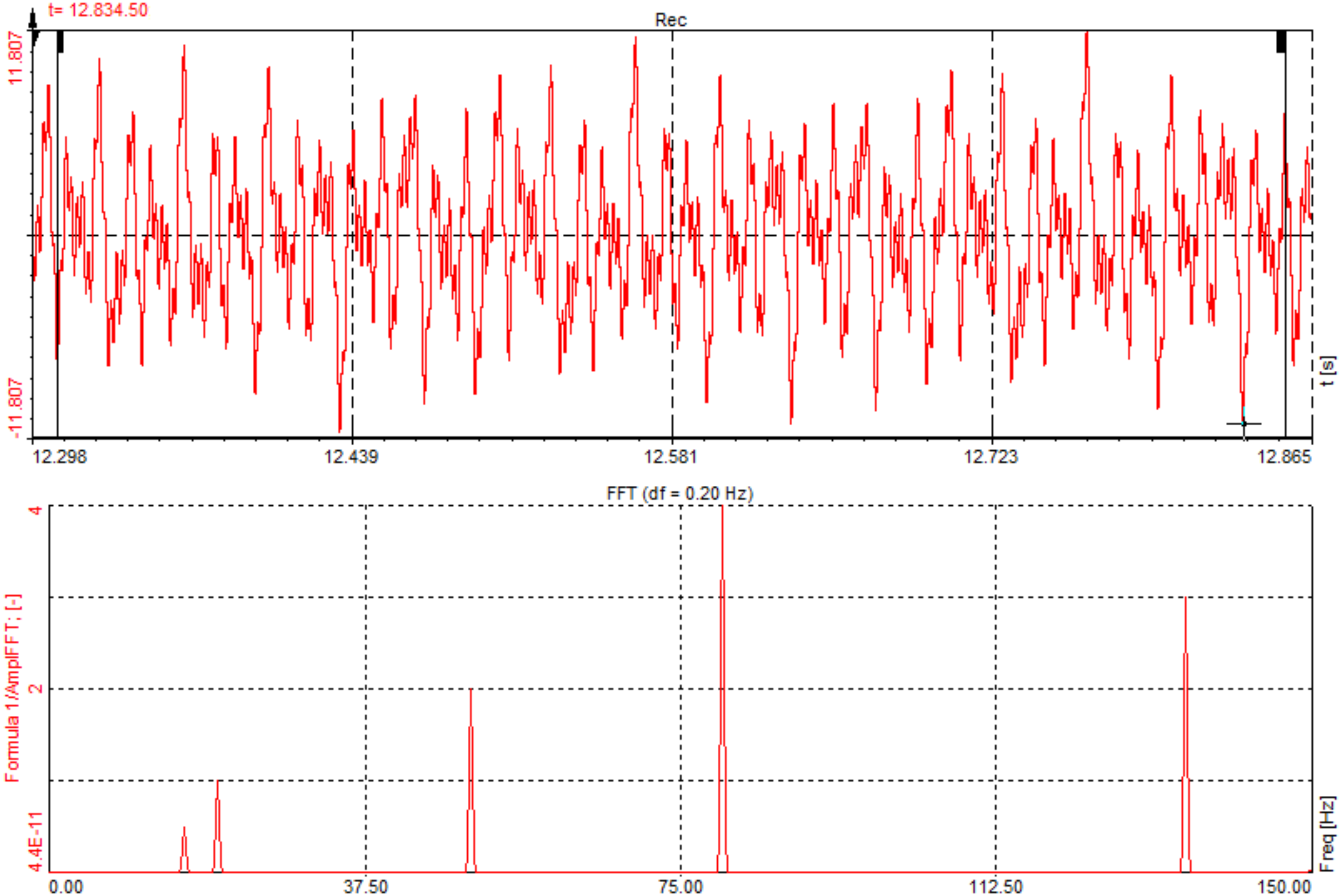

[redacted]

Power Spectrum of CMB Temperature Fluctuations

Sky map of CMBR temperature fluctuations

$$\Delta(\theta,\varphi)=\frac{T(\theta,\varphi)-\langle T\rangle}{\langle T\rangle}$$

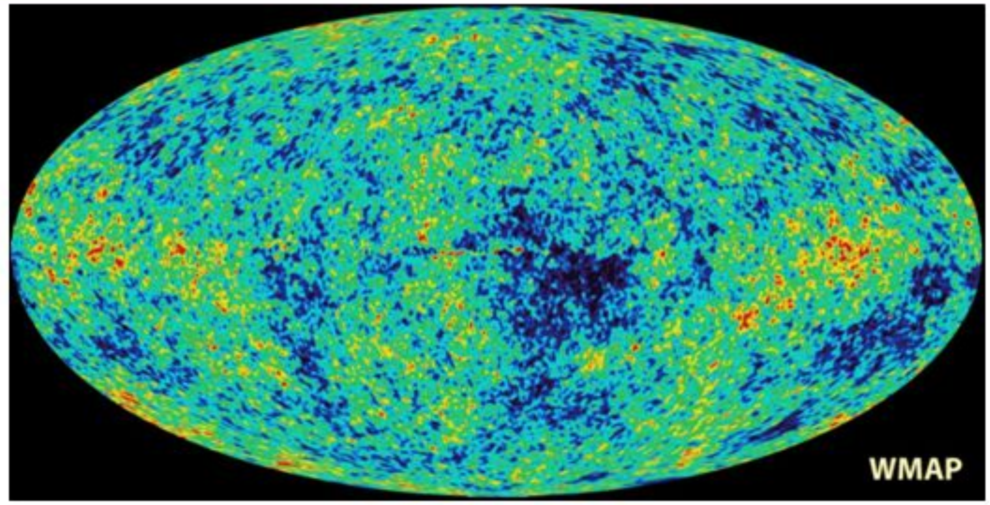

Multipole expansion

$$\Delta(\theta,\varphi)=\sum_{\ell=0}^{\infty}\sum_{m=-\ell}^{\ell}a_{\ell m}Y_{\ell m}(\theta,\varphi)$$

Angular power spectrum

$$C_\ell=\left\langle a_{\ell m}^{*}a_{\ell m}\right\rangle=\frac{1}{2\ell+1}\sum_{m=-\ell}^{\ell}a_{\ell m}^{*}a_{\ell m}$$

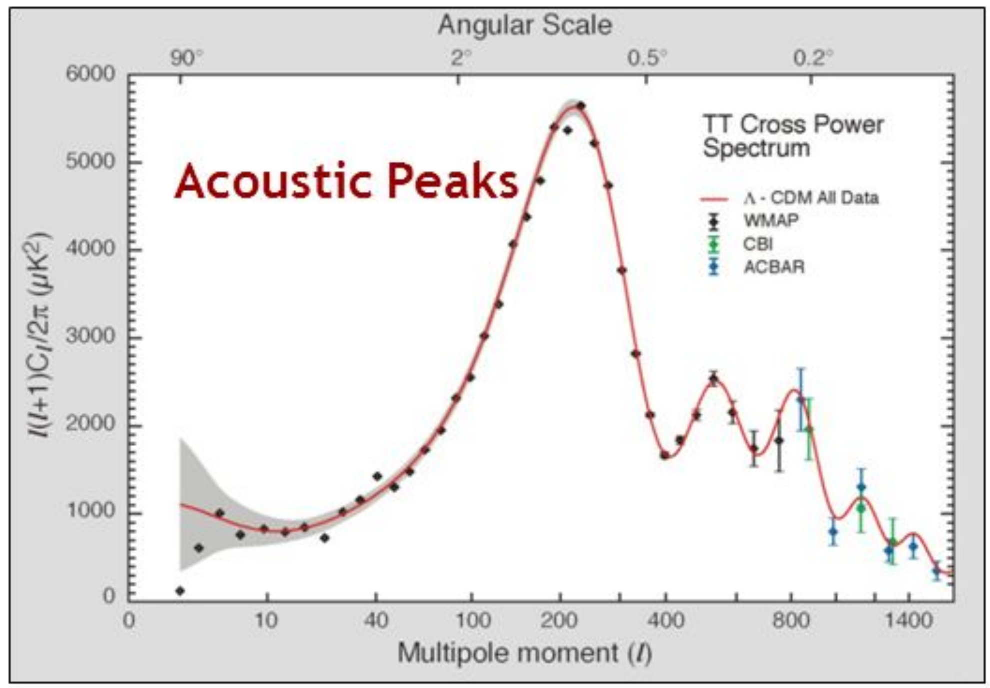

SPHERICAL HARMONICS

The spherical harmonics are given by

$$Y_{lm}(\theta,\varphi) = (-1)^m \left[\frac{2l+1}{4\pi}\frac{(l-m)!}{(l+m)!}\right]^{\frac{1}{2}} P_l^m(\cos\theta)e^{im\varphi}$$

For m>=0. and

$$Y_{l,-m} = (-1)^m Y_{lm}^*$$

The functions P^m_l are the associated Legendre polynomials defined by

$$P_l^m(u) = (-1)^{l+m}\frac{(l+m)!}{(l-m)!}\frac{(1-u^2)^{-m/2}}{2^l l!}\left(\frac{d}{du}\right)^{l-m}(1-u^2)^l$$

which is valid for m >= 0, and the values for negative m given by

$$P_l^{-m}(u) = (-1)^m\frac{(l-m)!}{(l+m)!}P_l^m(u)$$

(Remember $u = \cos\theta$).

Determine the values of

SPHERICAL HARMONICS

TABLE 6.5
The First Few Spherical Harmonics, $Y_J^m(\theta, \phi)$ [a]

$$Y_0^0 = \frac{1}{(4\pi)^{1/2}} \qquad Y_1^0 = \left(\frac{3}{4\pi}\right)^{1/2} \cos\theta$$

$$Y_1^1 = -\left(\frac{3}{8\pi}\right)^{1/2} \sin\theta e^{i\phi} \qquad Y_1^{-1} = \left(\frac{3}{8\pi}\right)^{1/2} \sin\theta e^{-i\phi}$$

$$Y_2^0 = \left(\frac{5}{16\pi}\right)^{1/2} (3\cos^2\theta - 1) \qquad Y_2^1 = -\left(\frac{15}{8\pi}\right)^{1/2} \sin\theta \cos\theta e^{i\phi}$$

$$Y_2^{-1} = \left(\frac{15}{8\pi}\right)^{1/2} \sin\theta \cos\theta e^{-i\phi} \qquad Y_2^2 = \left(\frac{15}{32\pi}\right)^{1/2} \sin^2\theta e^{2i\phi}$$

$$Y_2^{-2} = \left(\frac{15}{32\pi}\right)^{1/2} \sin^2\theta e^{-2i\phi}$$

a. The negative signs in $Y_1^1(\theta, \phi)$ and $Y_2^1(\theta, \phi)$ are simply a convention.

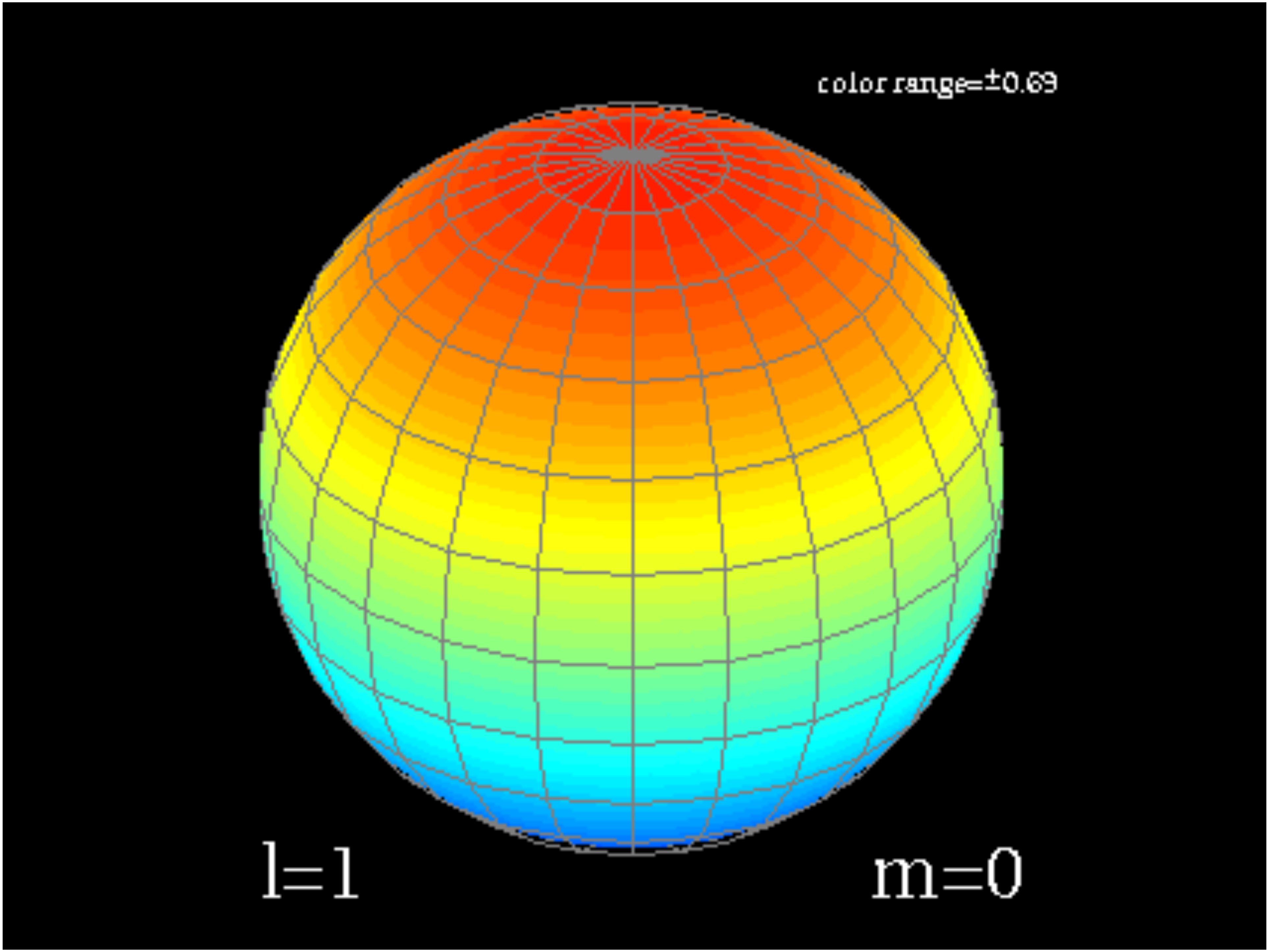
color range=±0.69
l=1
m=0

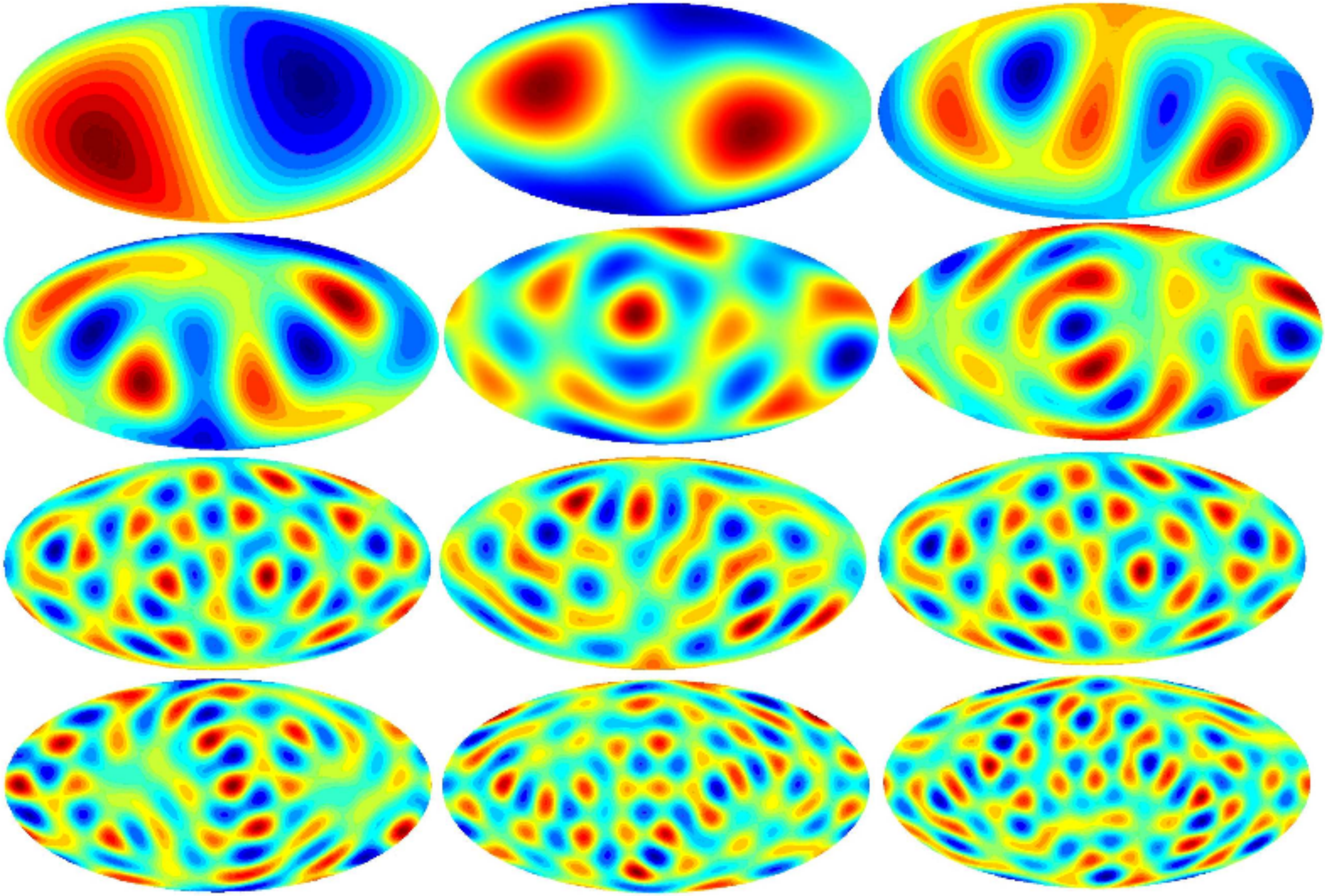

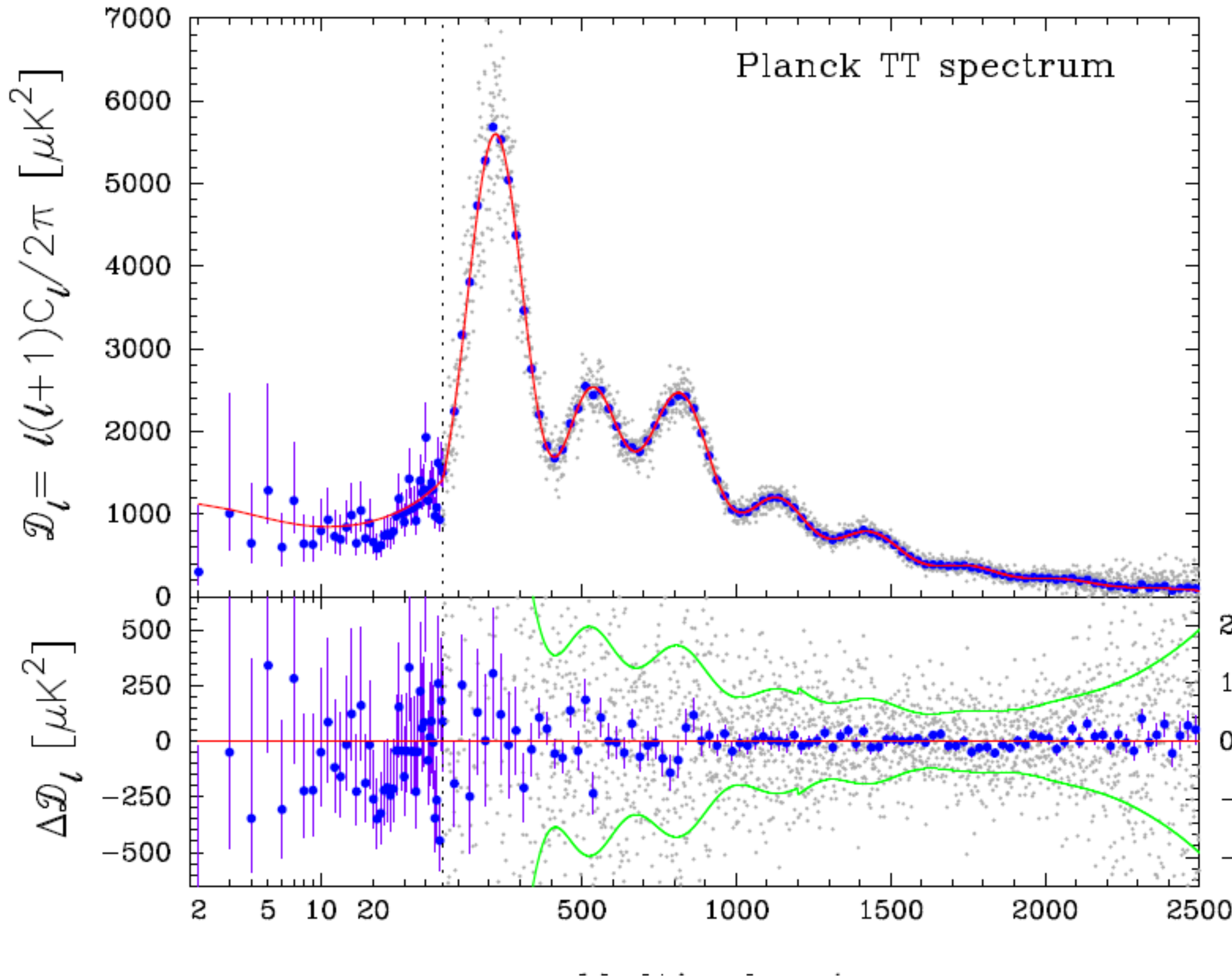

Planck TT spectrum
$\mathcal{D}_\ell = \ell(\ell+1)C_\ell/2\pi\ [\mu K^2]$
$\Delta\mathcal{D}_\ell\ [\mu K^2]$
7000
6000
5000
4000
3000
2000
1000
0
500
250
0
−250
−500
200
100
0
−100
−200
2
5
10
20
500
1000
1500
2000
2500

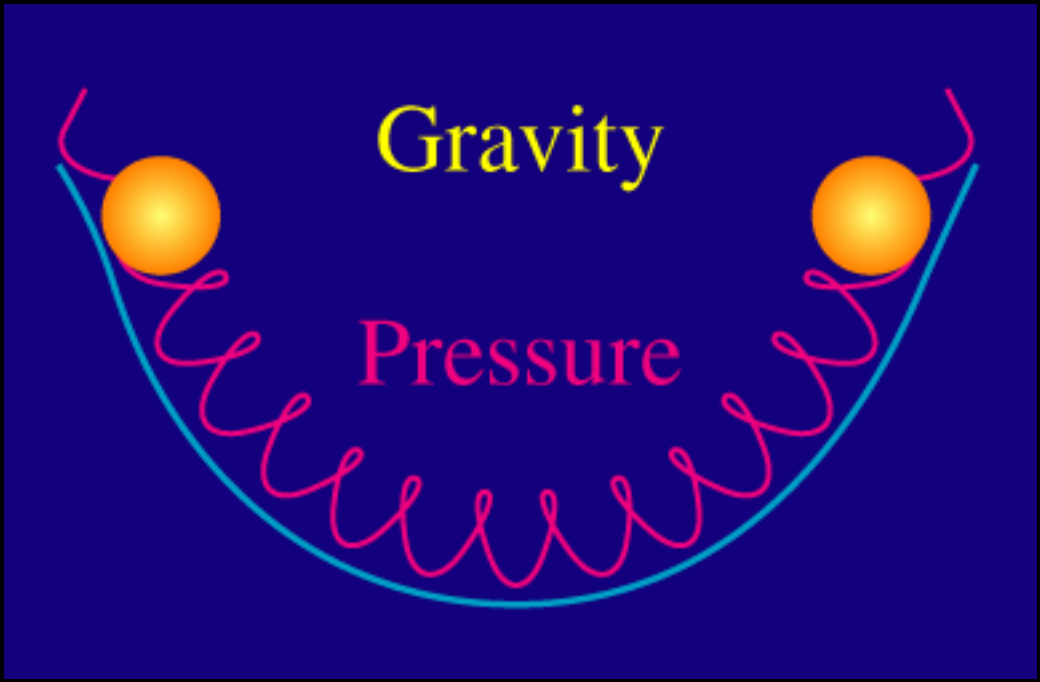

Dark Matter,
Baryons,
And Photons

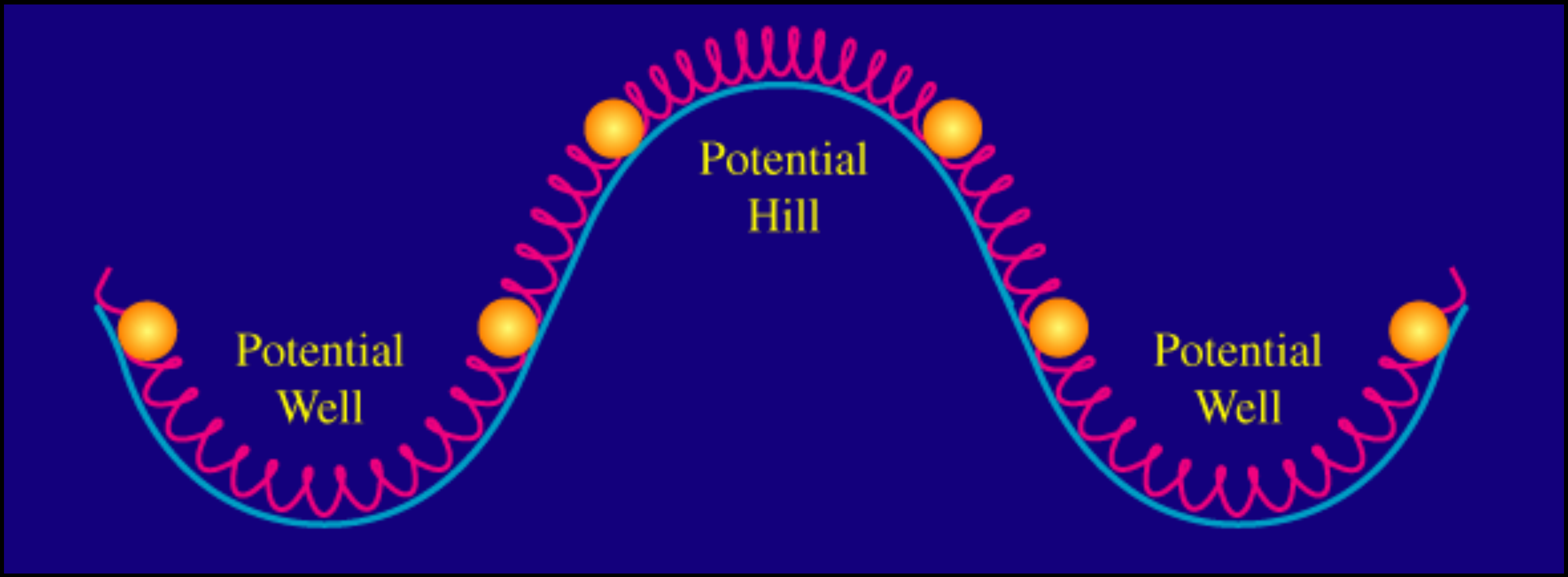

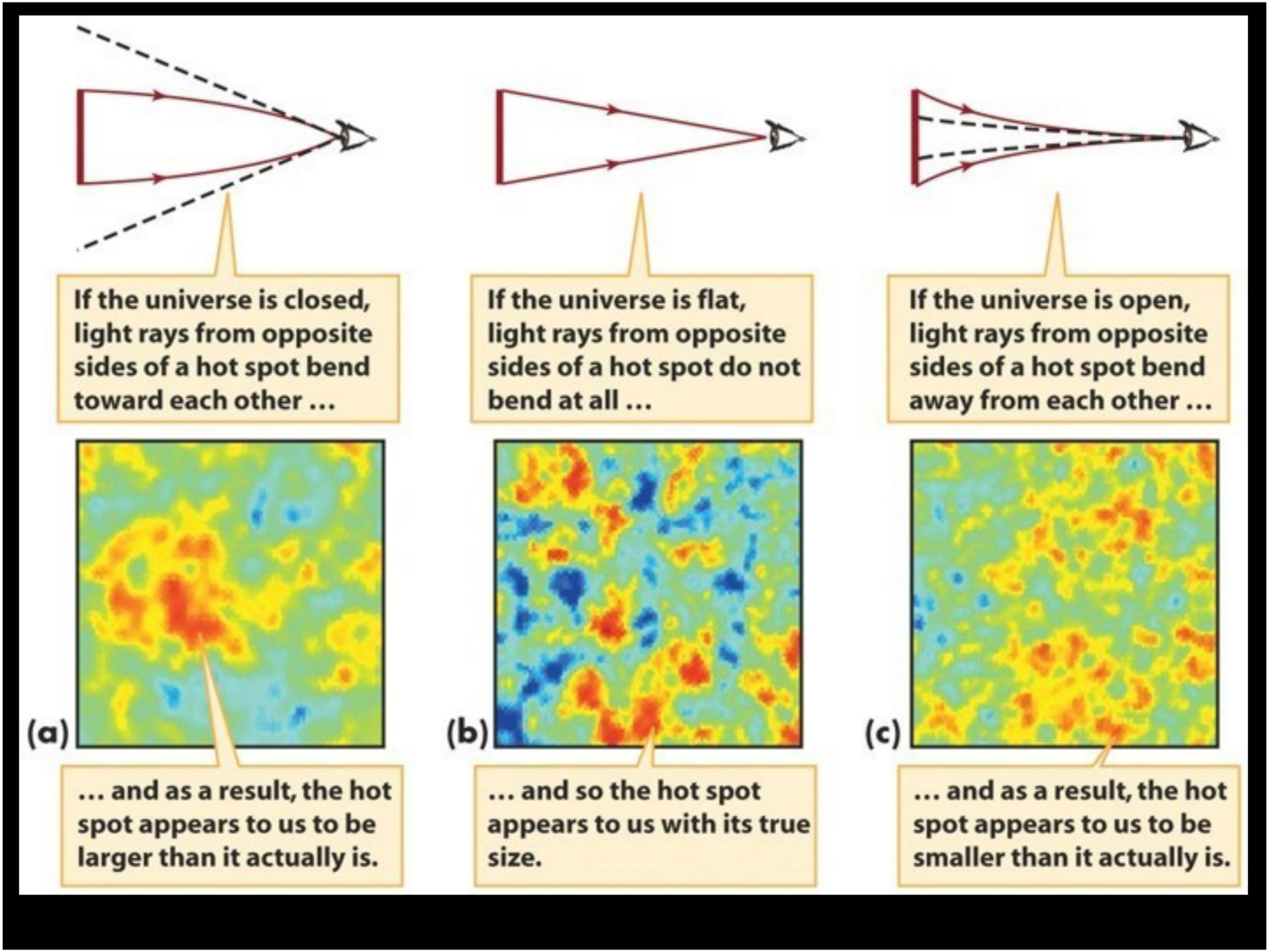
If the universe is closed, light rays from opposite sides of a hot spot bend toward each other …
If the universe is flat, light rays from opposite sides of a hot spot do not bend at all …
If the universe is open, light rays from opposite sides of a hot spot bend away from each other …
(a)
(b)
(c)
… and as a result, the hot spot appears to us to be larger than it actually is.
… and so the hot spot appears to us with its true size.
… and as a result, the hot spot appears to us to be smaller than it actually is.

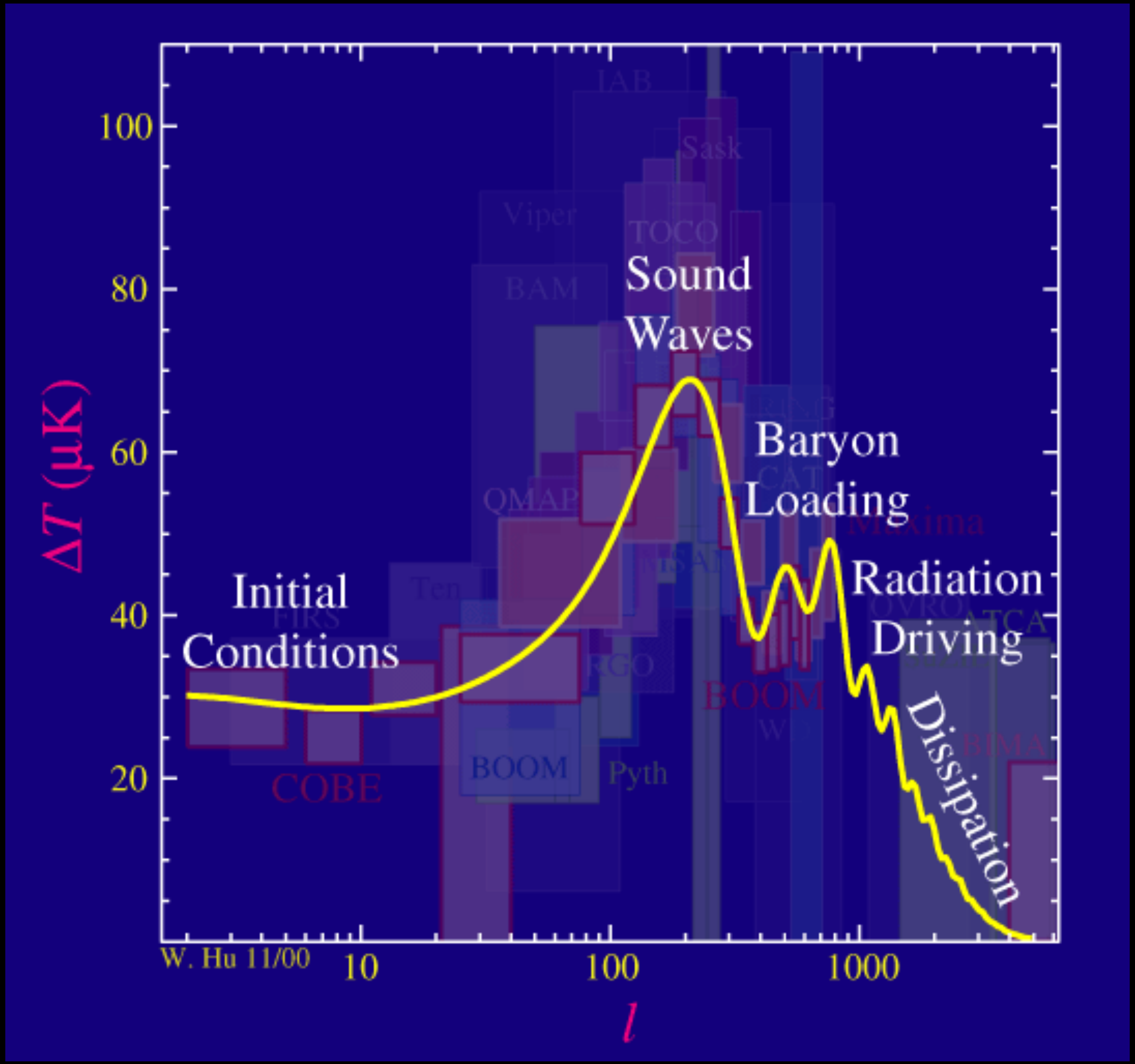

Acoustic Peaks

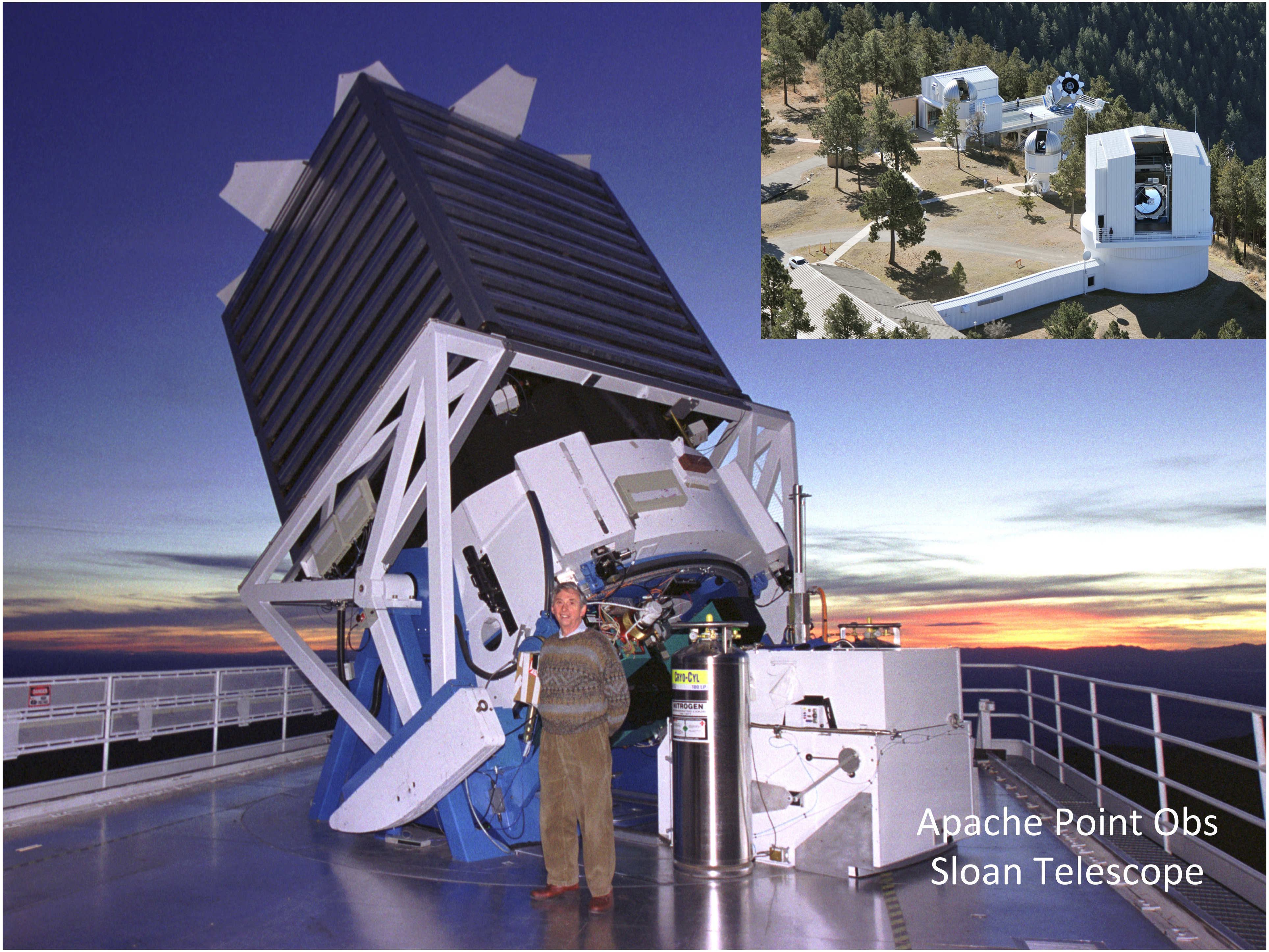
CRYO-CYL
NITROGEN
Apache Point Obs
Sloan Telescope

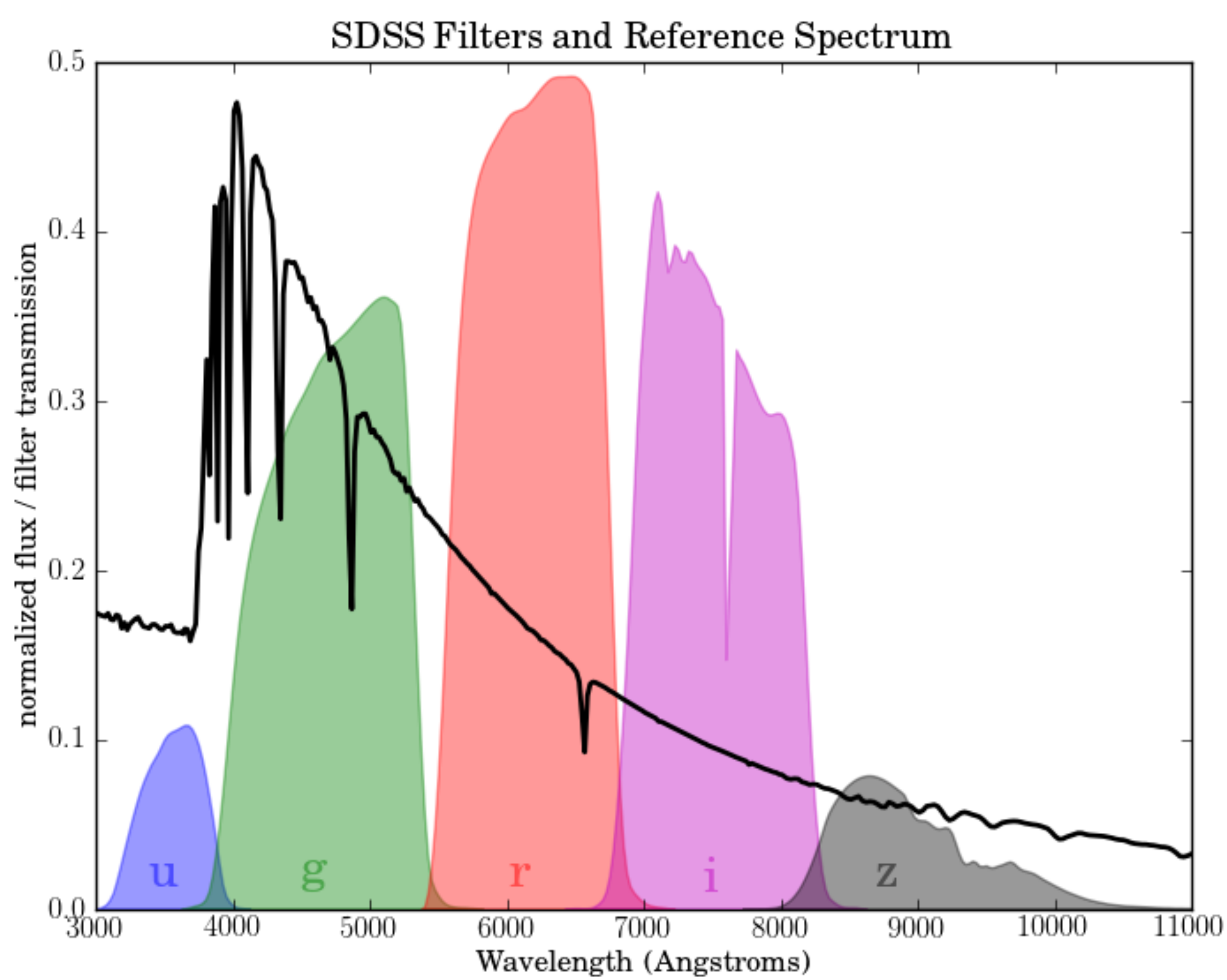

Sloan Filter Set

Two-Point Correlation Functions

Local density fluctuations are given by

$$\delta(x) = [\rho(x)-\rho_o(x)]/\rho_o(x),$$

where $\rho(x)$ is the local density and $\rho_o(x)$ is the average density. The two-point correlation function is then

$$\xi(x1,x2) = \langle\delta(x1)\cdot\delta(x2)\rangle$$

where x1 and x2 are two spatial locations. If the flucutatinos are uncorrelated then the expectations will be randomly distributed and the sums of $\xi(x1,x2)$ for fixed distances, s, between x1 and x2 average to 0, no correlation. If there is correlation then $\xi(s)$ may not be 0.

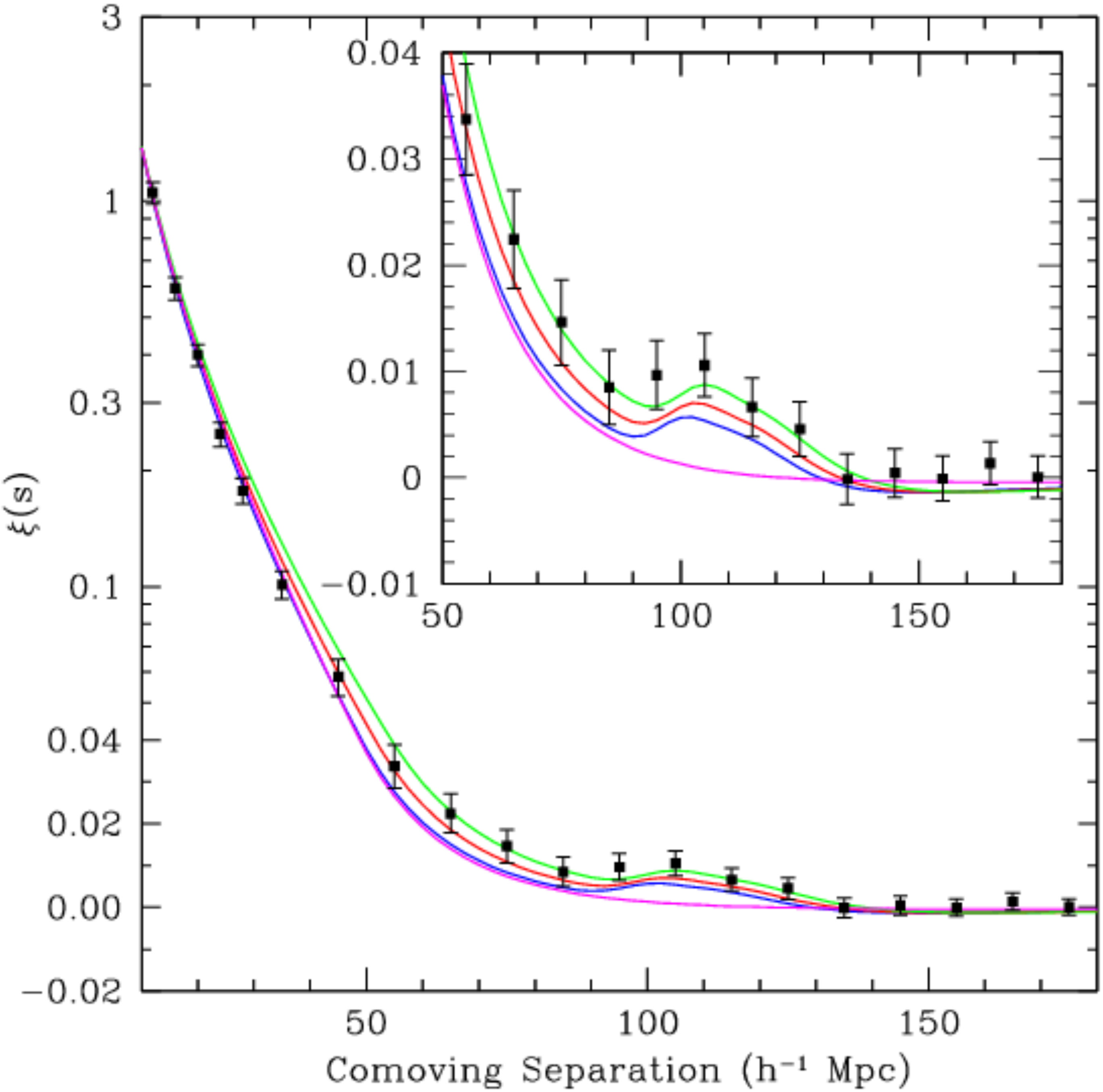

ξ(s)
Comoving Separation (h⁻¹ Mpc)
3
1
0.3
0.1
0.04
0.02
0.00
−0.02
50
100
150
0.04
0.03
0.02
0.01
0
−0.01

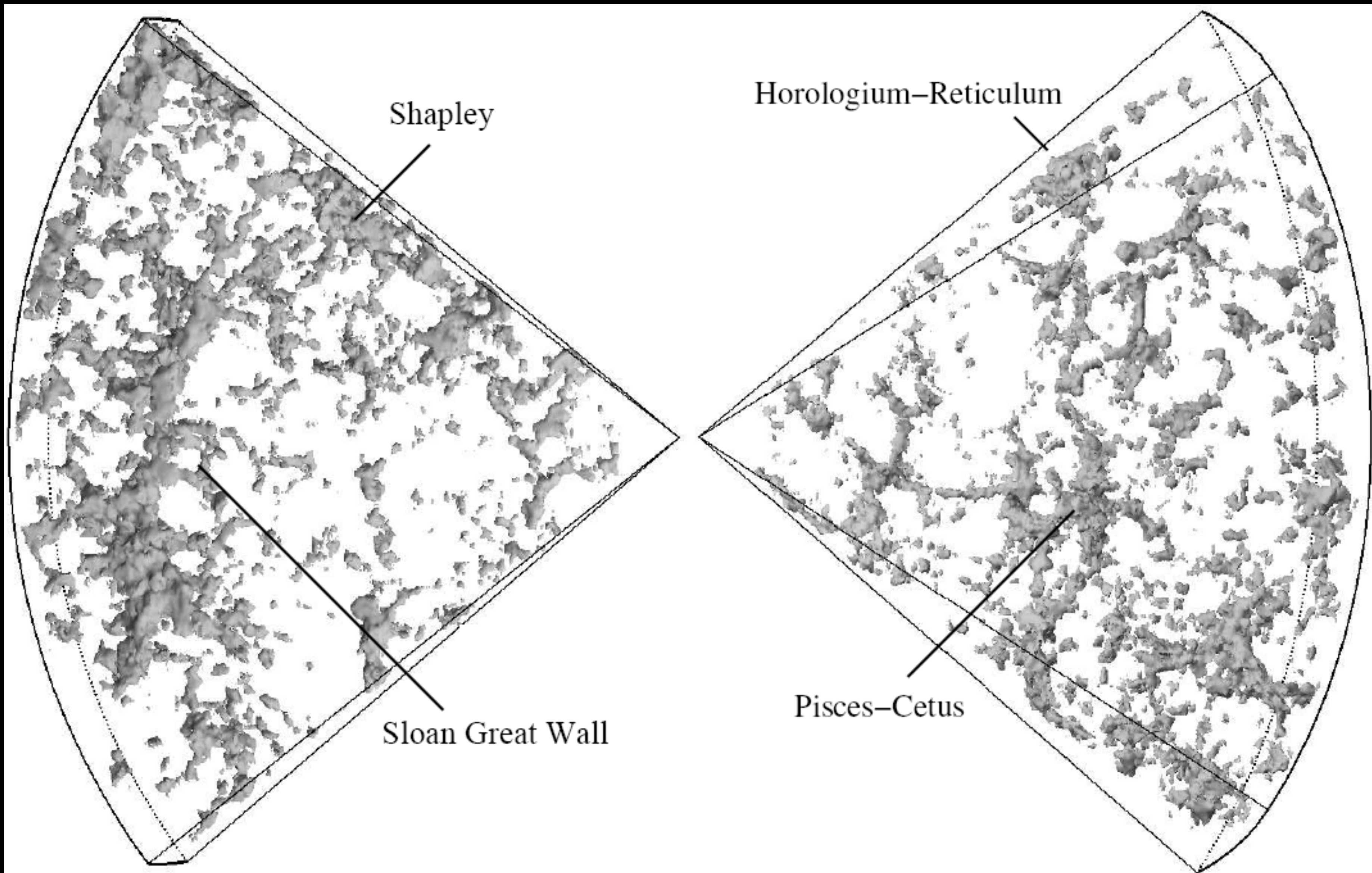
Shapley
Horologium–Reticulum
Sloan Great Wall
Pisces–Cetus

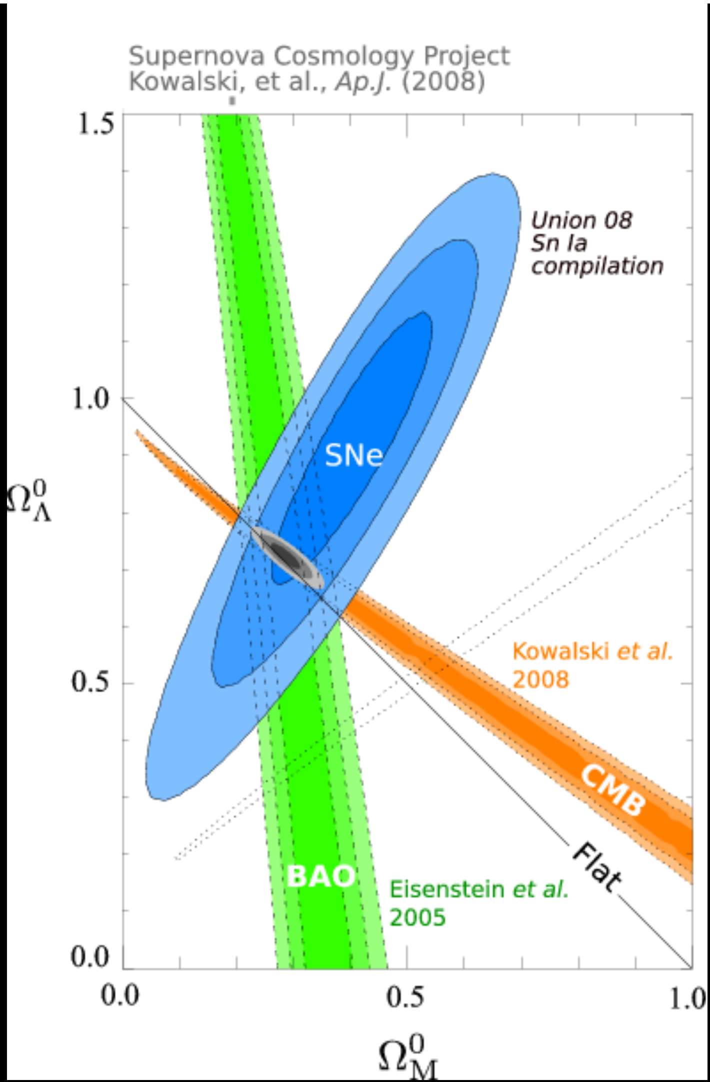

$$\left(\frac{\dot a}{a}\right)^2 \equiv H^2 = \frac{8\pi G}{3}\,\bar\rho + \frac{\Lambda}{3} - \frac{K}{a^2}\,; \quad (K = 0, \pm 1)\,, \qquad (17)$$

$$\frac{\ddot a}{a} = -\frac{4\pi G}{3}\,\bar\rho + \frac{\Lambda}{3}\,, \qquad (18)$$

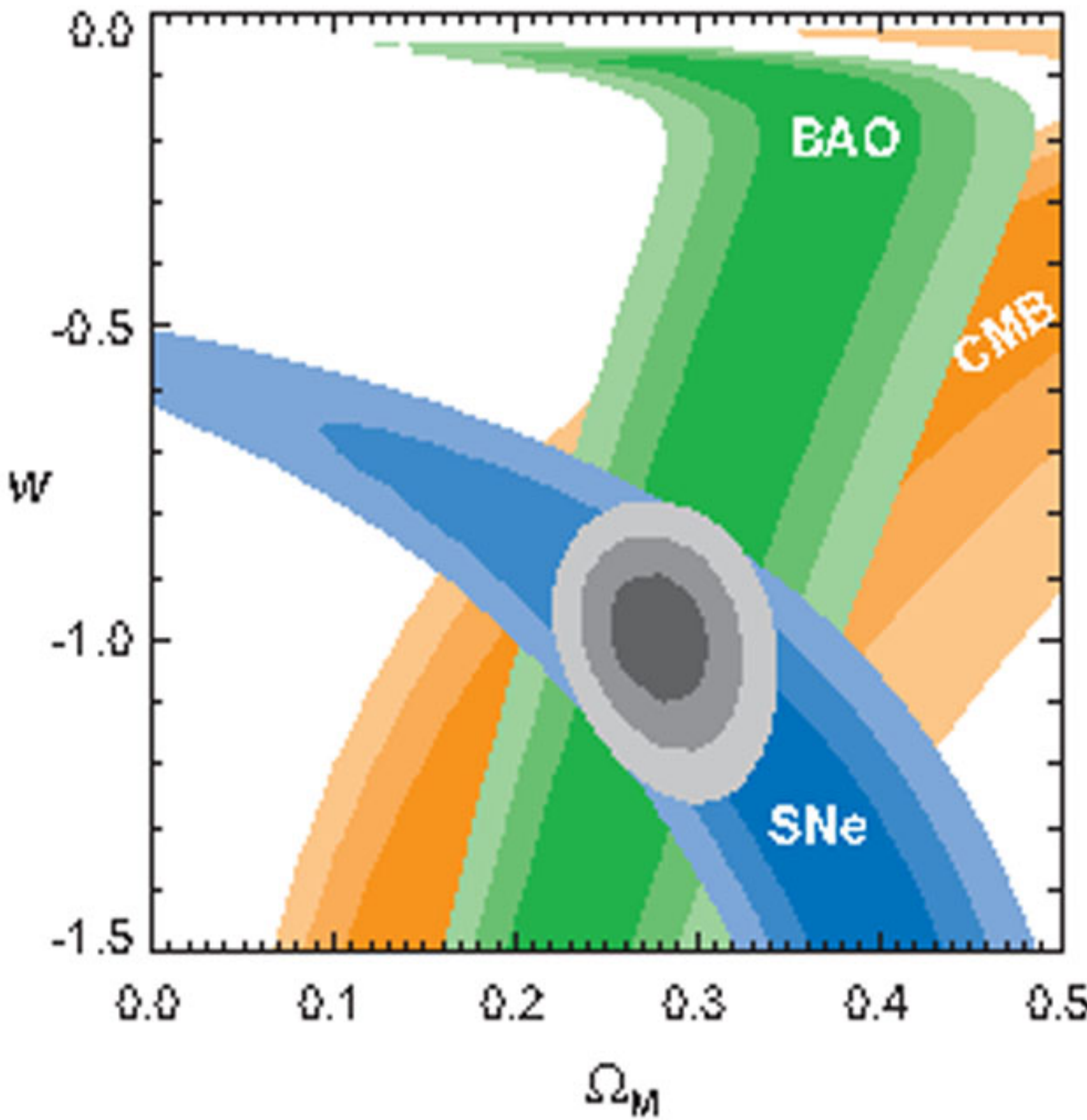
BAO
CMB
SNe
w
Ω_M
0.0
-0.5
-1.0
-1.5
0.0
0.1
0.2
0.3
0.4
0.5

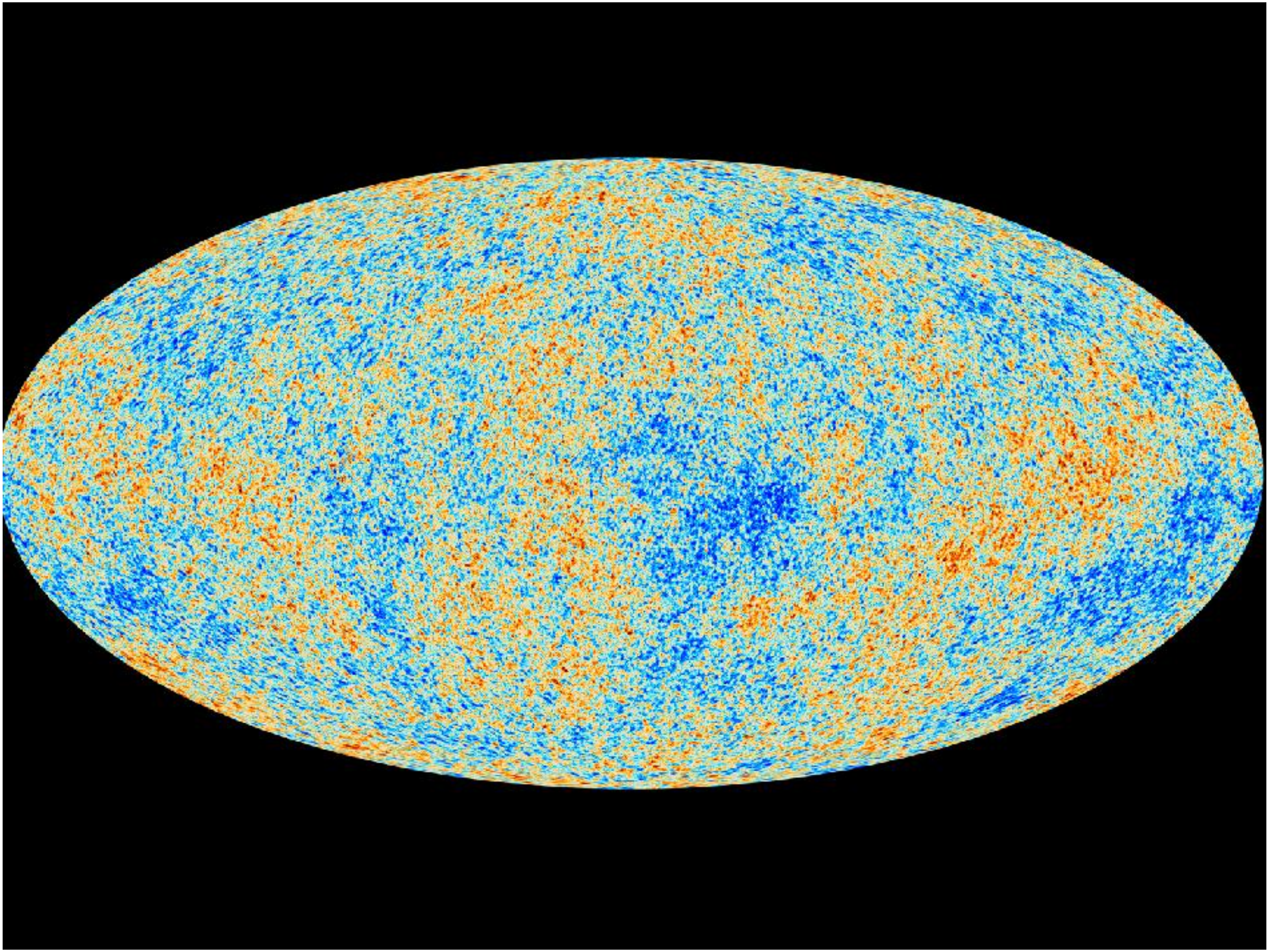

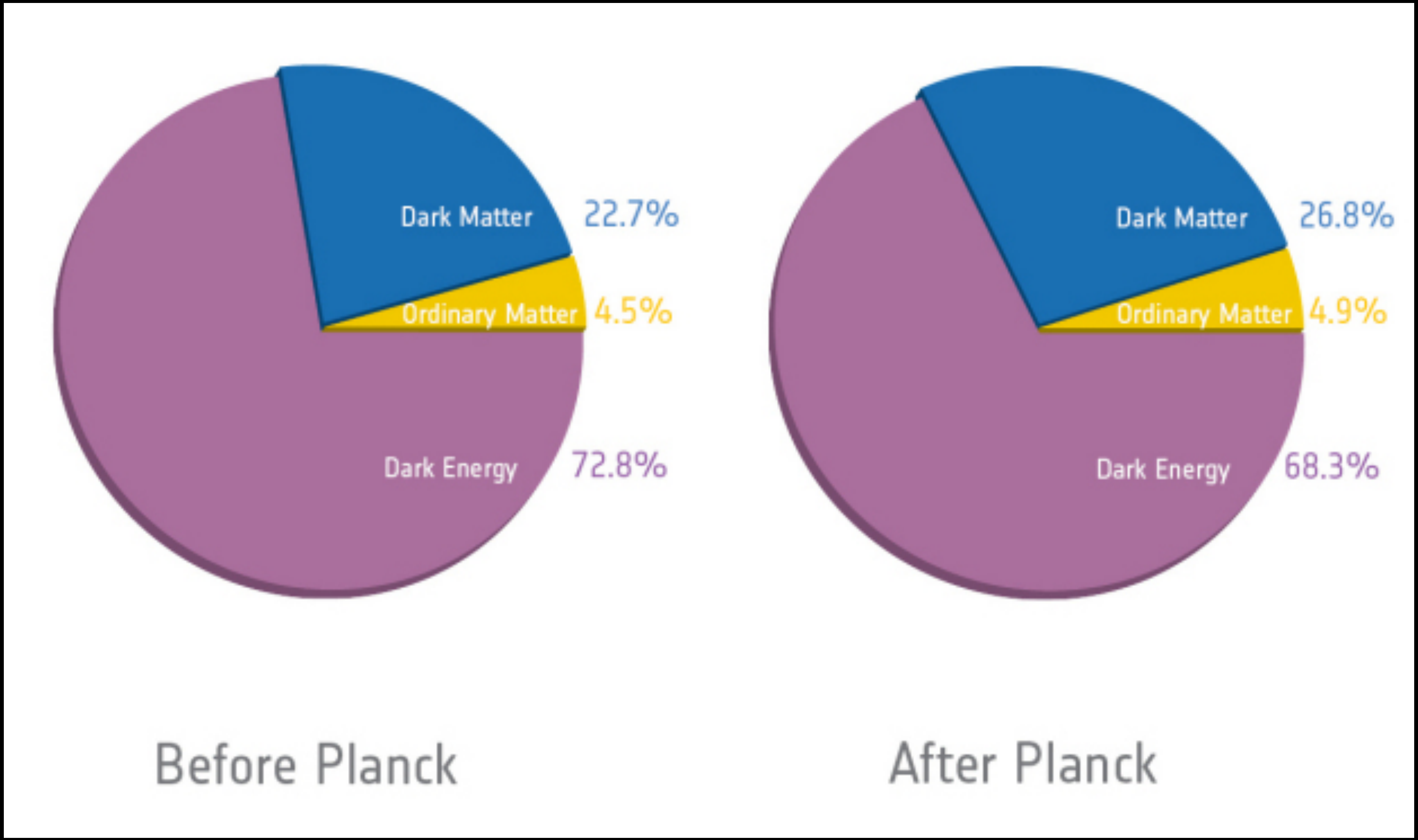
Dark Matter
22.7%
Ordinary Matter
4.5%
Dark Energy
72.8%
Before Planck
Dark Matter
26.8%
Ordinary Matter
4.9%
Dark Energy
68.3%
After Planck